WKB Analysis of PT-symmetric Hamiltonians

Bachelor's thesis

presented by

Philipp Oldigs

under the supervision of

Prof. Dr. Fabian Hassler
and
Prof. Dr. Markus Müller

Institute for Quantum Information RWTH Aachen

09 2026

Abstract

This thesis deals with the analysis of PT-symmetric Hamiltonians, using the WKB approximation. We elaborate on a formalism from prior work, which utilizes this approximation, to obtain a quantization condition for the spectra of the bound states of Hamilton operators $p^2 + V(q)$. The quantization condition of the semi-classical approximation proves to be capable of providing the spectrum beyond the PT-symmetry breaking of the states, as the potential is smoothly modified by a parameter. Furthermore, the understanding gained from the analysis is sufficient to trace back the PT-symmetry breaking to the actions between three turning points and allows us to calculate the critical parameter for the breaking of all states.

Contents

Abstract **iii**

1 Introduction **1**

2 WKB approximation **3**
2.1 Matching at the turning points 4
2.2 Complex continuation and Stokes phenomenon 6
2.2.1 Stokes phenomenon 6
2.2.2 Quantization condition 9
2.3 Complex potentials and Stokes graph 11
2.3.1 Branch cuts and tunneling 13

3 Analysis of PT-symmetric Potentials **15**
3.1 Numerical calculation of the Spectra with Hermite functions . . . 15
3.2 Potential $iq^3 + i\alpha q$ 16
3.2.1 Spectrum and eigenstates for $\alpha = 0$ 16
3.2.2 PT-symmetry breaking for $\alpha < 0$ 22
3.3 Potential $-iq^5 + i\alpha q$ 28
3.3.1 Spectrum for two pairs of turning points 28
3.3.2 PT-symmetry breaking 30

4 Conclusion and outlook **33**

A Additional figures **35**

Acknowledgements **41**

Declaration on the use of Artificial Intelligence **43**

List of Figures

2.1 Deformed contour in the complex plane 7
2.2 Circle around turning point with crossing of Stokes- and anti-Stokes line 8
2.3 Path around turning point with crossing of Stokes- and anti-Stokes line 9
2.4 Contour to solve the harmonic oscillator with Stokes-(dashed) and anti-Stokes lines(solid) as well as the dominant parts of the solution in the sectors 10
2.5 Sketch of the complete Stokes graph of the harmonic oscillator with dashed Stokes lines and solid anti-Stokes lines. 12

3.1 Sketch of the Stokes graph of iq^3 with solid anti-Stokes lines and dashed Stokes lines. 18
3.2 Ground state for $\alpha = 0$ with WKB approximation and the crossing of the Stokes lines 21
3.3 First excited state for $\alpha = 0$ with WKB approximation and the crossing of the Stokes lines 22
3.4 Turning points for increasing α with asymptotic anti-Stokes lines 23
3.5 Turning points for decreasing α and $\mathrm{Im}\, E > 0$ with asymptotic anti-Stokes lines 24
3.6 Sketch of the Stokes graph of iq^3 with solid anti-Stokes lines and dashed Stokes lines for $\alpha < \alpha_c$ 25
3.7 Sketch of the Stokes graph of iq^5 with solid anti-Stokes lines and dashed Stokes lines. 28
3.8 Turning points for positive α around the PT-symmetry breaking of the ground state 31

A.1 Sketch of the Stokes graph of $iq^3 + i\alpha q$ at $\alpha = -2.5 > \alpha_c$ with solid anti-Stokes lines and dashed Stokes lines. 35
A.2 Fit to $E_1(\alpha)^2 - E_0(\alpha)^2$ to determine $\alpha_c(0)$ 36
A.3 Fit to $E_3(\alpha)^2 - E_2(\alpha)^2$ to determine $\alpha_c(1)$ 36
A.4 Real part of ψ_2 for $\alpha < \alpha_c(1)$ 37
A.5 Real part of ψ_3 for $\alpha < \alpha_c(1)$ 37
A.6 Imaginary part of ψ_2 for $\alpha < \alpha_c(1)$ 38
A.7 Imaginary part of ψ_3 for $\alpha < \alpha_c(1)$ 38

List of Tables

3.1 Energies calculated with the quantization condition and numerically by expansion in the hermite basis 20
3.2 Comparison of $\alpha_c(n)$ for the different methods 28
3.3 Numerically calculated and WKB approximated energies for the contour γ_1 29

Chapter 1

Introduction

In standard quantum mechanics, the Hamiltonian of a system is required to be hermitian to provide a real spectrum and unitary time evolution. However, hermiticity is not a necessary condition and can be replaced by the weaker condition of PT-symmetry.

Since the observation that PT-symmetric Hamiltonians can have entirely real spectra in Ref.[1], PT-symmetric Hamiltonians and potentials have gained growing attention. These Hamiltonians occur in a wide range of problems. Examples are the propagation of light in a medium with a complex refractive index, where the optical wave equation is formally equal to the Schrödinger equation. In this field the first PT-symmetry breaking was experimentally observed in Ref.[2]. The observation of real energies for these Hamiltonians also enabled new theoretical approaches to problems like the Riemann hypothesis. A PT-symmetric Hamiltonian was constructed that has the imaginary parts of the nontrivial zeros of the Riemann zeta function as eigenvalues[3]. If these can be proven to be real the Riemann hypothesis would be confirmed.

Due to the versatile usage, it is of interest to get a better analytical understanding in this field. In this thesis we want to investigate PT-symmetric Hamiltonians with the WKB approximation. In the second chapter we will elaborate on a formalism with the approximation to construct a quantization condition, which will yield the approximated energies of the Hamiltonian. The presented formalism has already been used in Ref.[4] to investigate another PT-symmetric potential. Additionally, we will introduce the Stokes graph that will help to develop a deeper insight into the problem.

In the third chapter we will choose simple PT-symmetric potentials to apply the formalism to. We will analyze the PT-symmetry breaking of the states, induced by the change of a parameter in the potential. The structure of the turning points and the Stokes graph will help to clarify the process. The analysis of the Stokes graph will enable us to simplify the quantization condition to a few terms that cause the PT-symmetry breaking. From there, we will be able to determine the critical parameter for the PT-symmetry breaking of all states.

Chapter 2

WKB approximation

The WKB approximation, named after Wentzel, Kramers, and Brillouin, is a semiclassical approximation to solve the Schrödinger equation with a potential $V(q)$. We use the ansatz

$$\psi(q) = e^{\frac{i}{\hbar}S(q)} \tag{2.1}$$

with a complex function S for the state ψ, to solve the time-independent Schrödinger equation with the potential $V(q)$. q is already a rescaled variable with $q = \sqrt{2m}x$ so that the Schrödinger equation

$$-\hbar^2 \frac{d^2}{dq^2}\psi(q) = [E - V(q)]\,\psi(q) \tag{2.2}$$

follows. We substitute the ansatz and expand $S(q)$ in a series in $\hbar$ which yields

$$S(q) = S_0 + \hbar S_1 + \hbar^2 S_2 + \dots. \tag{2.3}$$

Keeping only the terms of zeroth and first order in $\hbar$ gives us two equations from (2.2)

$$S_0'^2 = E - V(q) = p(q)^2 \quad \text{an} \tag{2.4}$$

$$S_1' = \frac{iS_o''}{2S_0'} \tag{2.5}$$

The first two orders are a sufficient approximation as long as

$$\frac{\hbar|S_0''|}{|S_o'|^2} = \frac{i|p'(q)|}{p(q)^2} \ll 1 \tag{2.6}$$

holds. It can be shown that this corresponds to a slowly varying de-Broglie wavelength.

The equations (2.4) and (2.5) can be solved straightforwardly, yielding for the first two orders of $S(q)$,

$$S_0(q) = \pm\int_{q_r}^{q} \sqrt{E - V(\tilde{q})}\mathrm{d}\tilde{q} = \pm\int_{q_r}^{q} p(\tilde{q})\mathrm{d}\tilde{q} \tag{2.7}$$

$$\text{and} \quad S_1(q) = \frac{i}{2}\ln|S_0'| = \frac{i}{2}\ln|p(q)| \tag{2.8}$$

with an arbitrary reference point q_r. This brings our WKB approximation to

$$\psi(q) = \psi_+(q) + \psi_-(q) = \frac{C_+}{\sqrt{|S_0'(q)|}} e^{\frac{i}{\hbar}S_0(q)} + \frac{C_-}{\sqrt{|S_0'(q)|}} e^{-\frac{i}{\hbar}S_0(q)}. \tag{2.9}$$

C_+ and C_- are just some arbitrary constants.

The equation for the zeroth order, Eq.(2.4), is equal to the Hamilton-Jacobi-equation from classical mechanics so that we can identify $S_0(q)$ with the action between the reference point q_r and q.

If we first consider real, continuous potentials, we know that every potential with normalizable bound states must have at least two turning points where $E = V(q)$. At these we change from the classically allowed region to the classically forbidden region and vice versa. In the classically allowed region, $E > V(q)$, $p(q)$ is real so that $\psi(q)$ is purely oscillatory. In the classically forbidden region, $E < V(q)$, $p(q)$ is purely imaginary and $\psi_\pm(q)$ are exponentially increasing or decreasing.

The boundary condition of normalizable states restricts our solution in the classically forbidden region to the exponentially decreasing solution, which needs to be connected to the oscillatory solution at the turning points. The connection of the solutions with the boundary condition will give us a condition for the energies of the states. Close to a turning point q_0 we can expand the potential $V(q)$ into a power series and get

$$p(q)^2 \approx -V'(q_0)(q - q_0) \tag{2.10}$$

For $q \to q_0$, $p(q) \to 0$, so the condition Eq. (2.6) no longer holds and we cannot use the WKB approximated states, which would diverge at q_0. In contrast to this we know from theory that the solutions of the Schrödinger equation are analytic.

This problem requires a careful treatment of the wavefunction at the turning points and will be explained in the following.

2.1 Matching at the turning points

The conventional way of matching the wavefunctions between the classically allowed and forbidden region is to expand the potential in the Schrödinger equation. The expanded Schrödinger equation

$$\frac{d^2}{dq^2}\psi(q) = \frac{V'(q_0)}{\hbar^2}(q - q_0)\psi(q) \tag{2.11}$$

gives us the Airy equation which is solved by the well known Airy functions $c_A Ai(u) + c_B Bi(u)$ with $u = (|V'(q_0)|/\hbar^2)^{1/3}(q - q_0)$. The linearization of the potential remains valid for $q \gg q_0$ because for the expansion of $V(q)$ only the condition

$$|V''(q_0)(q - q_0)^2| \ll |V'(q_0)(q - q_0)| \Rightarrow u \ll \left(\frac{|V'(q_0)|}{\hbar^2}\right)^{1/3} \left|\frac{V'(q_0)}{|V''(q_0)}\right| \tag{2.12}$$

needs to hold, which is the case even for large u because $\hbar$ is arbitrarily small [5].

For two turning points q_1, q_2 on the real axis with $q_1 < q_2$ we will need to match the WKB solution with the Airy functions. At q_1 we switch from a region with $E < V(q)$ to $E > V(q)$, which means $V'(q_1) < 0$. When q approaches $-\infty$, $Bi(-u)$ diverges, so the coefficient c_B must be zero and the solution consists only of $Ai(-u)$. For $|u| \gg 1$ we can use the asymptotic expressions

$$u \ll -1 \Rightarrow Ai(-u) \sim \frac{1}{2|u|^{\frac{1}{4}}} e^{-\frac{2}{3}|u|^{\frac{3}{2}}} \tag{2.13}$$

$$u \gg 1 \Rightarrow Ai(-u) \sim \frac{1}{|u|^{\frac{1}{4}}} \cos\left(\frac{2}{3}|u|^{\frac{3}{2}} - \frac{\pi}{4}\right) \tag{2.14}$$

for $Ai(-u)$.

These expressions have to be matched with the WKB wavefunction with the linearized potential, which is given by

$$\psi(q \ll 1) = \frac{A}{|p(q)|^{\frac{1}{4}}} e^{\frac{2}{3}|u|^{\frac{3}{2}}} + \frac{B}{|p(q)|^{\frac{1}{4}}} e^{-\frac{2}{3}|u|^{\frac{3}{2}}} \tag{2.15}$$

$$\text{and } \psi(q \gg 1) = \frac{C}{|p(q)|^{\frac{1}{4}}} e^{i\frac{2}{3}|u|^{\frac{3}{2}}} + \frac{D}{|p(q)|^{\frac{1}{4}}} e^{-i\frac{2}{3}|u|^{\frac{3}{2}}}. \tag{2.16}$$

A comparison of both expressions yields for the coefficients $A = 0, B = \frac{1}{2}, C = ce^{-i\frac{\pi}{4}}$, and $D = ce^{i\frac{\pi}{4}}$, so that we have a condition for the general WKB solution at the first turning point with

$$\psi(q) = \frac{1}{2\sqrt{|p(q)|}} e^{-\frac{1}{\hbar}\int_q^{q_1} \sqrt{V(\tilde{q})-E}\,\mathrm{d}\tilde{q}} \quad \text{for } q < q_1 \tag{2.17}$$

$$\text{and } \psi(q) = \frac{c}{\sqrt{|p(q)|}} \cos\left[\frac{1}{\hbar}\int_{q_1}^{q} p(\tilde{q})\mathrm{d}\tilde{q} - \frac{\pi}{4}\right] \quad \text{for } q > q_1. \tag{2.18}$$

An analogous treatment at the second turning point with $V'(q_2) > 0$ yields

$$\psi(q) = \frac{1}{2\sqrt{|p(q)|}} e^{-\frac{i}{\hbar}\int_{q_2}^{q} p(\tilde{q})\mathrm{d}\tilde{q}} \quad \text{for } q > q_2, \tag{2.19}$$

$$\psi(q) = \frac{\tau c}{\sqrt{|p(q)|}} \cos\left[\frac{1}{\hbar}\int_{q}^{q_2} p(\tilde{q})\mathrm{d}\tilde{q} - \frac{\pi}{4}\right] \quad \text{for } q < q_2. \tag{2.20}$$

Because we require a solution where $\psi(q) \to 0$ for either $q \to -\infty$ or $q \to \infty$ and because the solution must be analytic, the terms of both turning points for the classically allowed region need to be identical. Therefore the condition

$$\cos\left[\frac{1}{\hbar}\int_{q_1}^{q} p(\tilde{q})\mathrm{d}\tilde{q} - \frac{\pi}{4}\right] = \tau \cos\left[\frac{1}{\hbar}\int_{q}^{q_2} p(\tilde{q})\mathrm{d}\tilde{q} - \frac{\pi}{4}\right] \tag{2.21}$$

follows, which can only be satisfied for $\tau = \pm 1$. A trivial calculation supplies for both τ

$$\sin\left[\frac{1}{\hbar}\int_{q_1}^{q_2} p(\tilde{q})\mathrm{d}\tilde{q} - \frac{\pi}{2}\right] = 0 \tag{2.22}$$

$$\Rightarrow \int_{q_1}^{q_2} p(\tilde{q})\mathrm{d}\tilde{q} = \hbar\pi\left(n + \frac{1}{2}\right). \tag{2.23}$$

This is the quantization condition for the energies of a potential with two real turning points. For more turning points on the real axis we can extend the matching of the solutions to more regions which will provide the quantization condition for more turning points.

The harmonic oscillator with the potential $V(q) = q^2$ has two turning points on the real axis at $\pm\sqrt{E}$. The integral in the quantization condition can be evaluated analytically and gives us

$$\int_{-\sqrt{E}}^{\sqrt{E}} \sqrt{E - q^2}\mathrm{d}q = E\frac{\pi}{2} \Rightarrow E\frac{\pi}{2} = \pi\hbar(n + \frac{1}{2}) \Rightarrow E = \hbar(2n + 1) \tag{2.24}$$

Thus, the WKB approximation produces the exact energies for this potential.

2.2 Complex continuation and Stokes phenomenon

For arbitrary potentials it is often more convenient to extend the problem to the complex plane and use a formalism that does not require the turning points to lie on the chosen contour.

The WKB solution diverges near a turning point and can not be used as seen above. By deforming the contour, for now the real axis, around the turning point like seen in Fig. 2.1, the WKB approximation holds on the entire contour. Instead of matching the different WKB solutions at the turning points with the Airy functions, we need to track our solution along the deformed contour through the complex plane and account for the Stokes phenomenon when moving around the turning point. As we will see, these two approaches are closely related.

2.2.1 Stokes phenomenon

The Stokes phenomenon describes that the asymptotic expansion of an analytic function is seemingly discontinuous when moving into regions of different asymptotic behavior.

The Stokes phenomenon occurs in our problem because the WKB approximation is an asymptotic expansion, which is multi-valued, for the entire, single-valued wavefunction. We see this effect when using the asymptotic Airy functions near our turning point. Considering a turning point of the same type as q_2, the solution for small positive u near the turning point is given by

$$\psi(u) \sim \frac{1}{u^{\frac{1}{4}}} e^{-\frac{2}{3}u^{\frac{3}{2}}}. \tag{2.25}$$

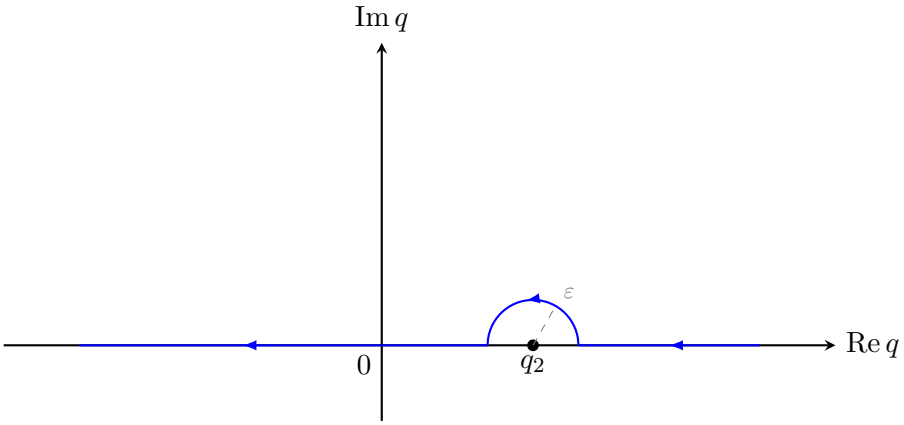


Figure 2.1: Deformed contour in the complex plane

If we follow this solution on our contour around the turning point, i.e. $u = re^{i\varphi}$ and $\varphi \in [0, \pi]$, we will get at $\varphi = \pi$

$$\psi(u) \sim \frac{e^{-i\frac{\pi}{4}}}{r^{\frac{1}{4}}} e^{\frac{2}{3}ir^{\frac{3}{2}}} \tag{2.26}$$

which is not equal to our known solution for $u < 0$ (2.14). An exponential term being of the same order as the already existing term is missing. It is not possible to recover this term from further corrections of the asymptotic expansion. Returning to the WKB approximation, an exponential term with an exponent of the order $\frac{1}{\hbar}$ would be missing, which can not be obtained from higher orders S_2, S_3. This means we need to include this term separately.

To analyze this effect in more detail, we will look at the exponent of our solution (2.25) while moving along the contour. The sign of the real part of the exponent is responsible for giving us an increasing or decreasing exponential function. Due to the boundary condition $c_+ = 0$ and $\psi = \psi_-$. ψ_- is a decreasing exponential and therefore subdominant. While moving around the turning point, the exponent of ψ_- changes and first becomes purely imaginary at $\varphi = \pi/3$ and then purely real but positive at $\varphi = 2\pi/3$. ψ_- becomes dominant. In this region ψ_+ is subdominant and at $\varphi = 2\pi/3$ it would only contribute within the error of the approximation. At $\varphi = \pi$ both solutions are purely oscillatory and so equally large. The lines where the solutions are purely oscillatory are called anti-Stokes lines, the lines where the solutions are purely exponentially increasing and decreasing are called Stokes lines.

This means when crossing a Stokes line in the complex plane, the coefficient of the subdominant part of the solution must be modified to get the right asymptotic solution in the adjacent region. This does not make the combined total solution discontinuous, since it is only an exponentially small term when added, but it can become significant when entering another region in the complex plane.

The change in the coefficient of the subdominant solution, when crossing a

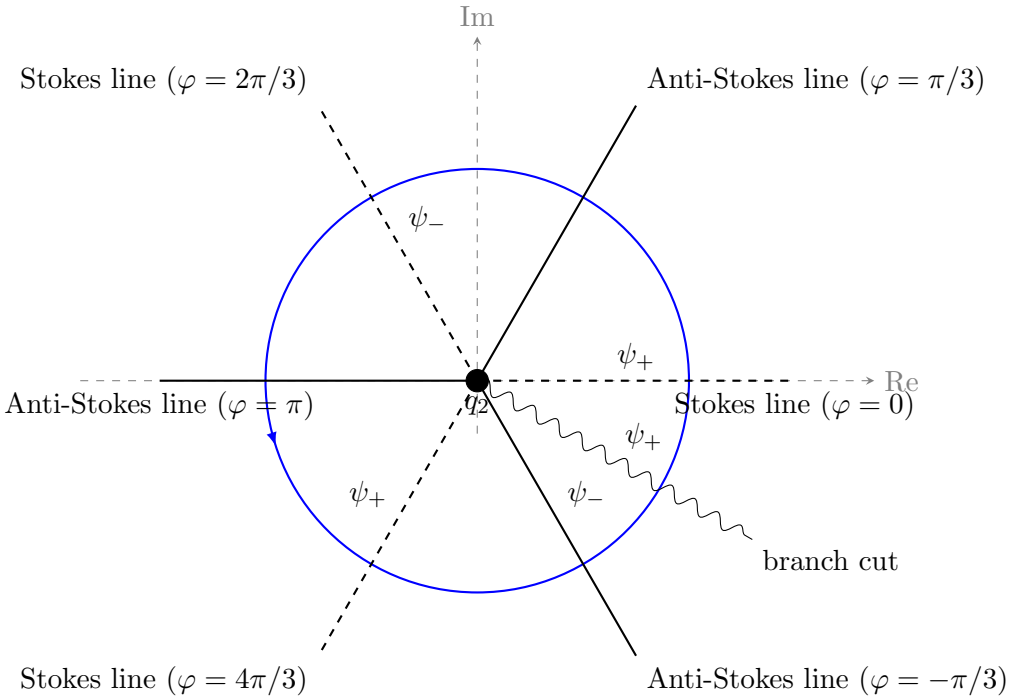


Figure 2.2: Circle around turning point with crossing of Stokes- and anti-Stokes line

Stokes line, can in general be expressed as

$$\psi = a\psi_+ + b\psi_- \to a\psi_+ + (b + \alpha a)\psi_-, \tag{2.27}$$

when ψ_- is subdominant. The constant α can be determined by demanding that after one full circuit around the turning point the solution stays the same.

It can be seen that ψ_-, Eq. (2.25), as well as ψ_+ with a switched sign in the exponent, have three Stokes lines at $\varphi = 0, \frac{2\pi}{3}, \frac{4\pi}{3}$ and three anti-Stokes lines at $\varphi = \frac{1\pi}{3}, \pi, \frac{5\pi}{3}$. Additionally, when moving around the closed path, we will cross the branch cut at some point. When crossing the branch cut the solutions change with $\psi_- \to -i\psi_+$ and $\psi_+ \to -i\psi_-$. The dominance structure of the solution remains the same and the sectors with the dominant solution can be seen in Fig. 2.2, with the chosen branch cut.

Starting at $\varphi = \pi/4$ with a general solution like seen in equation (2.27), we cross three Stokes lines and the branch cut before returning to $\varphi = 9\pi/4$. Using equation (2.27) at the Stokes lines, with different factors at different Stokes lines, produces

$$\psi = -i[a + \beta(b + \alpha a)]\psi_+ - i\{b + \alpha a + \gamma[a + \beta(b + \alpha a)]\}\psi_-. \tag{2.28}$$

This should be equal to the solution $\psi = a\psi_- + b\psi_+$. Comparing the coefficients of $\psi_\pm$ yields $\alpha = \beta = \gamma = i$.

The change in the coefficient of the subdominant solution corresponds to adding i times the coefficient of the dominant solution when moving over a Stokes line of a pole of our asymptotic solution counterclockwise. Clockwise would mean we need to add $-i$ times the coefficient of the dominant solution. A more complete derivation can be found in [6].

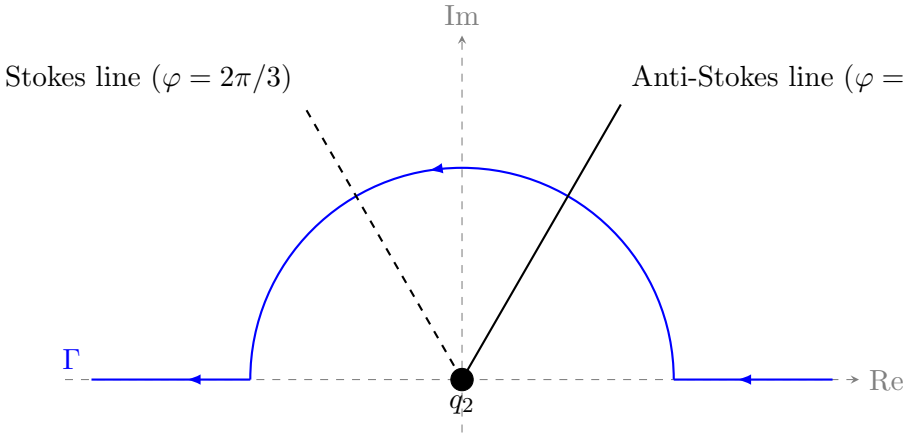


Figure 2.3: Path around turning point with crossing of Stokes- and anti-Stokes line

Going back to the example above, the connection over the Stokes line in Fig. 2.3 should now resolve the problem. At $\varphi = 0$, $\psi = 0\psi_+ + \psi_-$ and we cross only one Stokes line, where ψ_- is the dominant solution. At $\varphi = \pi$ the solution becomes

$$\psi(u) \sim e^{i\frac{\pi}{2}} \frac{1}{u^{\frac{1}{4}}} e^{\frac{2}{3}u^{\frac{3}{2}}} + \frac{1}{u^{\frac{1}{4}}} e^{-\frac{2}{3}u^{\frac{3}{2}}} \tag{2.29}$$

$$\sim \frac{1}{u^{\frac{1}{4}}} \cos\left(\frac{2}{3}u^{\frac{3}{2}} - \frac{\pi}{4}\right) \tag{2.30}$$

In the last step we used that $u \to -u$ when going around the contour. Disregarding global constants this provides the correct asymptotic solution on the other side of the turning point.

2.2.2 Quantization condition

Similar to above a normalizable wavefunction provides a quantization condition for the energies. The condition can now be obtained by moving along the contour through the complex plane and connecting the WKB solution across the Stokes lines.

Before we are able to achieve this, we need to set the arbitrary reference point in the WKB solution. The change of this point does not affect our solution because it creates just a constant factor. It is still very useful to set this reference point to the turning points. The modification of the wavefunction when crossing a Stokes line has only the simple form of equation (2.27) if the WKB approximation has the reference point set to the turning point that belongs to the crossed

Stokes line. This is because the simple connection formula is derived with the Airy-functions, which represent the local behavior around the turning point. For other reference points equation (2.27) would not hold and the connection would need to be derived for every crossing.

This means each time before crossing a Stokes line, we need to switch the reference point of our WKB approximation to the suitable turning point. This will supply constant factors in front of ψ_+ and ψ_- that are related to the classical action between these points and will come up in the quantization condition. Because the asymptotic of the Airy function is equal to the WKB approximation for the linearized potential near the turning points, we already know from above, Fig. 2.2, that each turning point will have three Stokes lines and three anti-Stokes lines emerging. These lines need to be considered when moving around the turning point.

As an example we will solve the energies of the harmonic oscillator using this alternative approach.

The turning points are at $q_{2/1} = \pm\sqrt{E}$, so that we now need to calculate the directions in which the Stokes lines emerge. To do this we linearize the potential and analyze the exponent of our WKB solution. For $V(q) = q^2$ we get

$$\psi(q) \sim e^{\pm\frac{i}{\hbar}\int_{q_2}^{q} p(\tilde{q})\mathrm{d}\tilde{q}} \sim e^{\pm\frac{i}{\hbar}\int_{q_2}^{q}\sqrt{-2q_2(\tilde{q}-q_2)}\mathrm{d}\tilde{q}} \sim e^{\mp\frac{1}{\hbar}\sqrt{2q_2}(q-q_2)^{\frac{3}{2}}} \tag{2.31}$$

We can see that the Stokes lines emerge at angles of $0, \frac{2\pi}{3}, \frac{4\pi}{3}$ from the turning point. For the turning point q_1 they emerge at the angles $\frac{\pi}{3}, \pi, \frac{5\pi}{3}$. Moreover we can see that with $(q-q_2)^{\frac{3}{2}} = r^{\frac{3}{2}}e^{i\frac{3}{2}\varphi}$, for $\varphi \in [-\frac{\pi}{3}, \frac{\pi}{3}]$, ψ_- is the dominant part of the solution and ψ_+ the subdominant part. For $\varphi \in [\frac{\pi}{3}, \pi]$, the dominance changes. At the point q_1 the structure is mirrored with respect to the imaginary axis.

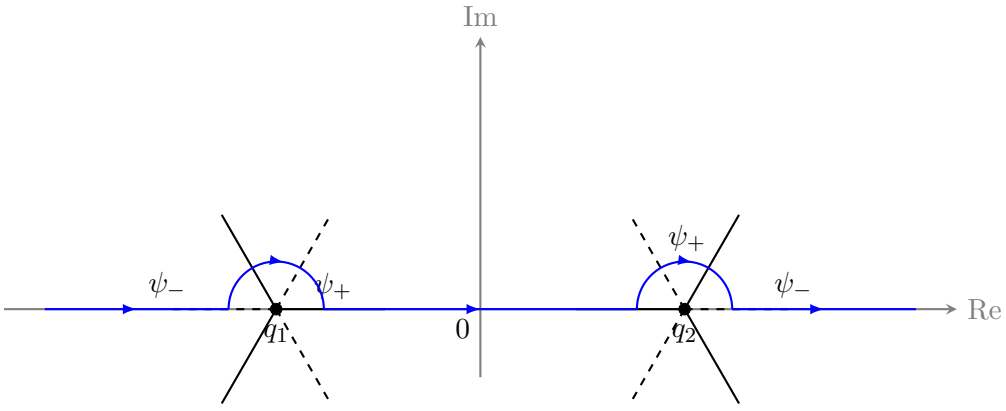


Figure 2.4: Contour to solve the harmonic oscillator with Stokes-(dashed) and anti-Stokes lines(solid) as well as the dominant parts of the solution in the sectors

We can choose a contour that goes around the turning points, seen in Fig. 2.4, and track our WKB solution along the way, including the continuation across

the Stokes lines. We see that at both turning points we cross one Stokes line at which the solution must be modified.

We begin at $q \to -\infty$ where we have the WKB solution $\psi(q) = \psi_+(q)$ with

$$\psi_+ = \frac{C}{p(q)^{\frac{1}{2}}} e^{iS_1(q)}, \quad \text{where} \quad S_1(q) = \frac{1}{\hbar}\int_{q_1}^{q} p(\tilde{q})\mathrm{d}\tilde{q}, \tag{2.32}$$

which is normalizable. When continuing on the contour, passing the first anti-Stokes line, the dominances change and ψ_+ is the dominant part of the solution. Then at the Stokes-line the coefficient of ψ_- changes with $-i$ times the coefficient of ψ_+. Therefore we have $\psi = \psi_+ - i\psi_-$. Before crossing the second Stokes-line at q_2 we need to change the reference point of our WKB approximation to q_2. To keep our approximated state unchanged we write $\psi_\pm$ as

$$\psi_\pm = \frac{C}{p(q)^{\frac{1}{2}}} e^{\pm iS_{1,2}} e^{\pm iS_2(q)} \tag{2.33}$$

$$\text{with} \quad S_2(q) = \frac{1}{\hbar}\int_{q_2}^{q} p(\tilde{q})\mathrm{d}\tilde{q} \quad \text{and} \quad S_{1,2} = \frac{1}{\hbar}\int_{q_1}^{q_2} p(q)\mathrm{d}q, \tag{2.34}$$

so that the state remains the same, just the coefficient and the exponential part transformed with

$$Ce^{\pm iS_{1,2}} = C_\pm. \tag{2.35}$$

Now we can cross the second Stokes line where ψ_+ is still dominant so the coefficient of ψ_- changes again. We get $\psi = C_+\psi_+ - i(C_+ + C_-)\psi_-$ and afterwards move over the anti-Stokes-line, so that now as $q \to \infty$, ψ_+ is again subdominant. The boundary condition demands that $-i(C_+ + C_-) = 0$ because otherwise ψ would not be normalizable. The condition simplifies to

$$\begin{aligned} C_+ + C_- = 0 \Rightarrow e^{iS_{1,2}} + e^{-iS_{1,2}} = 0 \Rightarrow 2\cos\left[S_{1,2}\right] = 0 \\ \Rightarrow S_{1,2} = (n + \frac{1}{2})\pi, \end{aligned} \tag{2.36}$$

which is the same condition we have found above by matching our solution with the Airy functions and which yields the exact energy levels of the harmonic oscillator.

Because $p(q)$ is analytic in the upper half plane, we also could have chosen any other way through the upper plane to determine the condition, like one semicircle through the upper plane enclosing both of the turning points. This would not affect the form of the quantization condition and so the energies.

2.3 Complex potentials and Stokes graph

For general complex potentials the turning points are located at arbitrary positions in the complex plane. If we want to calculate the WKB approximated energies along any contour, that does not go through a turning point, we can use the second method. For the quantization condition we need to determine

which Stokes lines, originating from which turning points, cross our contour in what order. As discussed the Stokes lines emerge from the turning points but afterwards are some curves in the complex plane defined by the condition $\mathrm{Re}\left[\int_{q_i}^{q} p(\tilde{q})\mathrm{d}\tilde{q}\right] = 0$. So it is not trivial to determine all Stokes curves associated with all turning points, which we combine in the Stokes graph.

To construct the Stokes graph we can analyse the initial directions of the Stokes lines, by expanding the potential at the turning points like done before for the harmonic oscillator. We can also expand $p(q)$ for $|q| \gg 1$, which gives us the asymptotic Stokes- and anti-Stokes lines which each Stokes- and anti-Stokes line needs to approach. Also we know that Stokes lines can not cross other Stokes lines, which reduces the possibilities of which Stokes line approaches which asymptotic line.

For the harmonic oscillator we want to investigate the asymptotic Stokes lines to get more information about the whole Stokes graph. For large $|q|$ we can expand

$$e^{\pm\frac{i}{\hbar}\int_{q_i}^{q}\sqrt{E-\tilde{q}^2}\mathrm{d}\tilde{q}} \sim e^{\mp\frac{1}{\hbar}\int_{q_i}^{q}\tilde{q}\mathrm{d}\tilde{q}} \sim e^{\mp\frac{1}{\hbar}r^2e^{2i\varphi}}, \tag{2.37}$$

so that we can see that the Stokes lines need to approach the angles $\varphi = 0, \frac{\pi}{2}, \pi, \frac{3\pi}{2}$ and the anti-Stokes lines the angles $\varphi = \frac{\pi}{4}, \frac{3\pi}{4}, \frac{5\pi}{4}, \frac{7\pi}{4}$. Also we can determine again, which component of the WKB approximation is dominant and subdominant, consistent with the dominances near the turning points.

If this information is not sufficient, we can always find the Stokes lines numerically by solving the condition for a Stokes line in the complex plane. For the harmonic oscillator the Stokes graph looks as shown in Fig. 2.5.

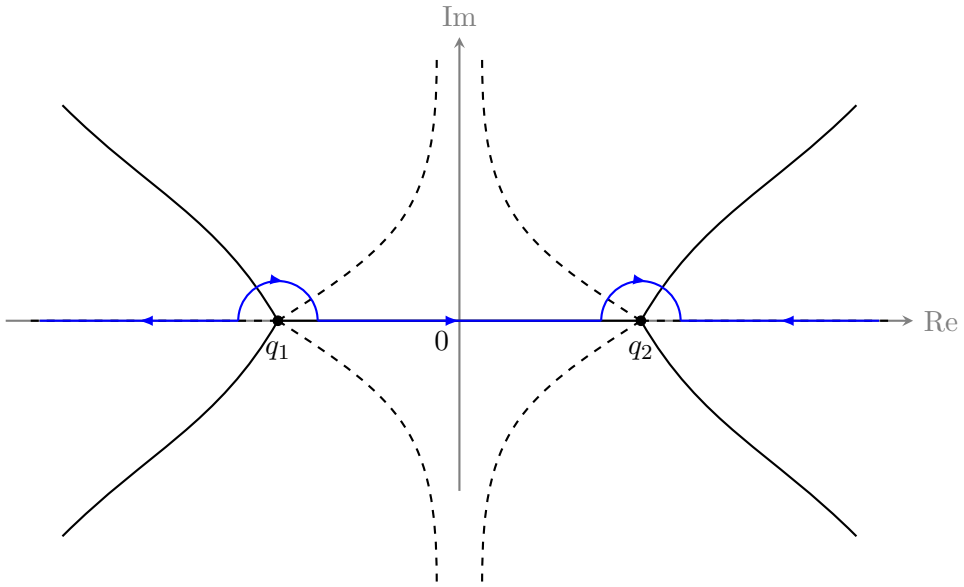


Figure 2.5: Sketch of the complete Stokes graph of the harmonic oscillator with dashed Stokes lines and solid anti-Stokes lines.

With the complete Stokes graph, we can calculate the quantization condition

for any contour and so the approximated energy levels for the states on this contour. It is straightforward to verify that for different contours that start and end in the same region, bounded by anti-Stokes lines, the quantization condition has the same form. Therefore the spectrum will be identical. In contrary, the wavefunctions may differ between different contours in the same asymptotic sectors.

2.3.1 Branch cuts and tunneling

For complex potentials and contours in the complex plane, we also need to take branch points and branch cuts of $p(q)$ into account. Every turning point, as well as ∞, is a branch point of $p(q)$. Normally, we can choose our branch cuts in such a manner that our contour does not cross any of them, but we need to be careful when calculating the actions $S_{i,j}$ and $S_0(q)$. In general, these actions are now defined by integrals in the complex plane, and their value can change when $p(q)$ switches to another branch unnoticed. Away from these branch cuts, $p(q)$ is analytic, so that the value of S only depends on the starting and ending points of the integral.

Another advantage of the second method presented here is that for contours that do not pass through a turning point, contributions from all turning points will be included in the quantization condition. For the matching with the Airy-functions, we would need to deform our contour through all relevant turning points. As we will see later for the explicitly analyzed potentials, the turning points lying in the same Stokes sector as the asymptotics will contribute in leading order to the quantization condition, whereas the other turning points contribute exponentially small corrections. The corrections can be identified as a possible tunneling of the particle to the turning points not lying in the sector.

Chapter 3

Analysis of PT-symmetric Potentials

In this chapter, we will use the introduced method to analyse PT-symmetric potentials with the complex WKB approximation and show that the semiclassical approximation can produce PT-symmetry breaking of states. The presented formalism was shown to be effective for the potential $q^4 + iAq$ in Ref. [4].

PT-symmetric potentials that are not hermitian but invariant under parity inversion and time reversal (PT) represent an infinite class of potentials, beside the normally analyzed, hermitian potentials. The PT-operator $\mathcal{PT}$ acts by the transformations $q \to -q$ and $i \to -i$. One can show with a simple calculation that the spectrum either consists of real energies E with PT-symmetric eigenstates ψ, fulfilling $\mathcal{PT}\psi = \psi$, or of pairs of complex conjugate energies with $H\psi = E\psi$ and $H(\mathcal{PT}\psi) = E^*(\mathcal{PT}\psi)$. For many cases all eigenstates are PT-symmetric, so we say they have an unbroken PT-symmetry. As we will see later on, continuous changes in the potential can break this symmetry and create the mentioned complex conjugate pairs of energies.

Eigenstates with an unbroken PT-symmetry have positive norms and an unitary time evolution, from which we gain access to the probability interpretation and other physical conclusions similar to hermitian quantum mechanics [7].

3.1 Numerical calculation of the Spectra with Hermite functions

To validate our results regarding the spectrum of the Hamiltonians and to help with the analysis of the Stokes sectors, we will expand our wavefunctions in the Hermite basis to calculate the energies and the eigenstates numerically.

The Hermite functions are given by

$$\Phi_n(q) = \frac{1}{\sqrt{2^n n! \sqrt{\pi}}} H_n(q) e^{-\frac{q^2}{2}}$$

where $H_n(q)$ is the n-th Hermite polynomial $H_n(q) = (-1)^n e^{q^2} \frac{d^n}{dq^n} e^{-q^2}$. The Hermite functions form a complete orthonormal system in $L^2(\mathbb{R})$, which is needed for the expansion of our eigenstates but will not be proven here. Therefore the eigenstates $\psi(q)$ can be written as

$$\psi(q) = \sum_{n=0}^{\infty} c_n \Phi_n(q)$$

Because the Hermite-basis has an infinite number of basis elements and we can not calculate an infinitely large matrix, we need to choose a cutoff N which restricts our number of eigenvalues and eigenstates. The Hermite functions are located around zero for small n, so the cutoff also determines that only states and the corresponding energies, which are located in this region of the real axis, can be covered by this calculation.

The position and momentum operators can be expressed by the ladder operators a and $a^\dagger$ which act on the Hermite functions according to the relations

$$q = \frac{(a + a^\dagger)}{\sqrt{2}}, \quad p = \frac{i(a^\dagger - a)}{\sqrt{2}} \tag{3.1}$$

$$a\,|\Phi_n\rangle = \sqrt{n}\,|\Phi_{n-1}\rangle, \quad a^\dagger\,|\Phi_n\rangle = \sqrt{n+1}\,|\Phi_{n+1}\rangle \tag{3.2}$$

so that we can write our Schrödinger equation in the Hermite basis with the matrices a and $a^\dagger$ and the eigenstates ψ

$$a \mathrel{\hat{=}} \begin{pmatrix} 0 & \sqrt{1} & 0 & 0 & \dots & 0 \\ 0 & 0 & \sqrt{2} & 0 & \dots & 0 \\ \vdots & \vdots & \vdots & \ddots & \dots & 0 \\ 0 & 0 & 0 & \dots & \sqrt{N-2} & 0 \\ 0 & 0 & 0 & \dots & 0 & \sqrt{N-1} \\ 0 & 0 & 0 & \dots & 0 & 0 \end{pmatrix}, \qquad |\psi\rangle \mathrel{\hat{=}} \begin{pmatrix} c_0 \\ c_1 \\ c_2 \\ \vdots \\ c_{N-1} \end{pmatrix} \tag{3.3}$$

This reduces the determination of the energies and eigenstates to an eigenvalue problem of a $N \times N$ matrix, which we can evaluate numerically with a simple Python code.

3.2 Potential $iq^3 + i\alpha q$

The first analyzed potential is $V(q) = iq^3 + i\alpha q$.

3.2.1 Spectrum and eigenstates for $\alpha = 0$

To get a better understanding of the potential, we first consider $\alpha = 0$ in which case we can obtain most of the results with the WKB method analytically.

The turning points are given by the solutions of the equation $E - V(q) = 0$ which is solved for $V(q) = iq^3$ by

$$q_n = E^{\frac{1}{3}} e^{\frac{i\pi}{3}(2n+\frac{3}{2})} \tag{3.4}$$

We want to focus on the energy levels of the states on the real axis. We can choose the real axis as our contour without any deformation because all turning points are located away from the real axis. For the quantization condition we need to determine the Stokes graph, at least around the real axis, to know which Stokes lines we cross and which solution is dominant when crossing this Stokes line.

First of all we will look again at the asymptotic Stokes and anti-Stokes lines for $|q| \gg 1$. We can expand our potential in $p(q)$ and get

$$\psi \sim e^{\pm i \int \sqrt{E-V(q)}\mathrm{d}q} \sim e^{\pm i \int \sqrt{-iq^3}\mathrm{d}q} \sim e^{\pm e^{\frac{i\pi}{4}} q^{\frac{5}{2}}} \tag{3.5}$$

[1] With the solutions of $\mathrm{Im}\left(e^{i\pi/4}q^{5/2}\right) = 0$ we obtain the asymptotic Stokes lines and with $\mathrm{Re}\left(e^{i\pi/4}q^{5/2}\right) = 0$ the asymptotic anti-Stokes lines that are the boundaries of the Stokes sectors.

With $q = re^{i\varphi}$ the equations yield that the anti-Stokes lines need to approach angles $\varphi = \frac{\pi}{10}, \frac{\pi}{2}, \frac{9\pi}{10}, \frac{13\pi}{10}, \frac{17\pi}{10}$ in the complex plane. The Stokes lines approach angles shifted by $\frac{\pi}{5}$. Because of the PT-symmetry of the potential, these asymptotic Stokes lines are symmetric to the imaginary axis as well as the complete Stokes graph.

Next we want to determine the local behavior of the Stokes lines around the turning points. As seen before we expand the potential around the turning points and get $V(q) \sim iq_n^3 + 3iq_n^2(q - q_n)$. We plug the potential into our WKB solution

$$\psi \sim e^{\pm i\sqrt{-3iq_n^2} \int \sqrt{q-q_n}\mathrm{d}q} \sim e^{\pm e^{i\frac{\pi}{4}} \sqrt{3q_n^2}(q-q_n)^{\frac{3}{2}}} \tag{3.6}$$

and solve the conditions for Stokes lines and anti-Stokes lines. In general the angles θ_n, at which the Stokes lines emerge from the turning points q_n, depend on the turning points themselves and therefore implicitly on the energies. For this potential we expect the energies to be real, as we can verify from our numerical calculation with the hermite basis, so that the phase of q_n and the angles θ_n are independent of the energies.

For the three turning points the angles θ_n are then given by the solutions of equation (3.7) and for the angles of the anti-Stokes lines γ_n by equation 3.8.

$$\sin(\frac{3}{2}\theta_n + \frac{\pi}{3}(2n + \frac{3}{2}) + \frac{\pi}{4}) = 0 \tag{3.7}$$

$$\cos(\frac{3}{2}\gamma_n + \frac{\pi}{3}(2n + \frac{3}{2}) + \frac{\pi}{4}) = 0 \tag{3.8}$$

[1] From now on we will set $\hbar$ to 1 by changing our system of units.

To further extend our knowledge about the Stokes graph, we will calculate numerically, how many Stokes lines of each turning point cross the real axis. For this we only need to find the solutions of

$$\mathrm{Im}\, i \int_{q_n}^{q} \sqrt{E - V(\tilde{q})}\mathrm{d}\tilde{q} = 0 \tag{3.9}$$

with regards to $q \in \mathbb{R}$. The number of Stokes lines that cross the contour, with the dominance of the solutions at these lines, determines the quantization condition we get. With substitution, the energy dependence only appears as a factor in front of q in the upper limit. For the number of roots this dependence is irrelevant.

This information is sufficient for the quantization condition and even allows us to sketch the whole Stokes graph in Fig. 3.1.

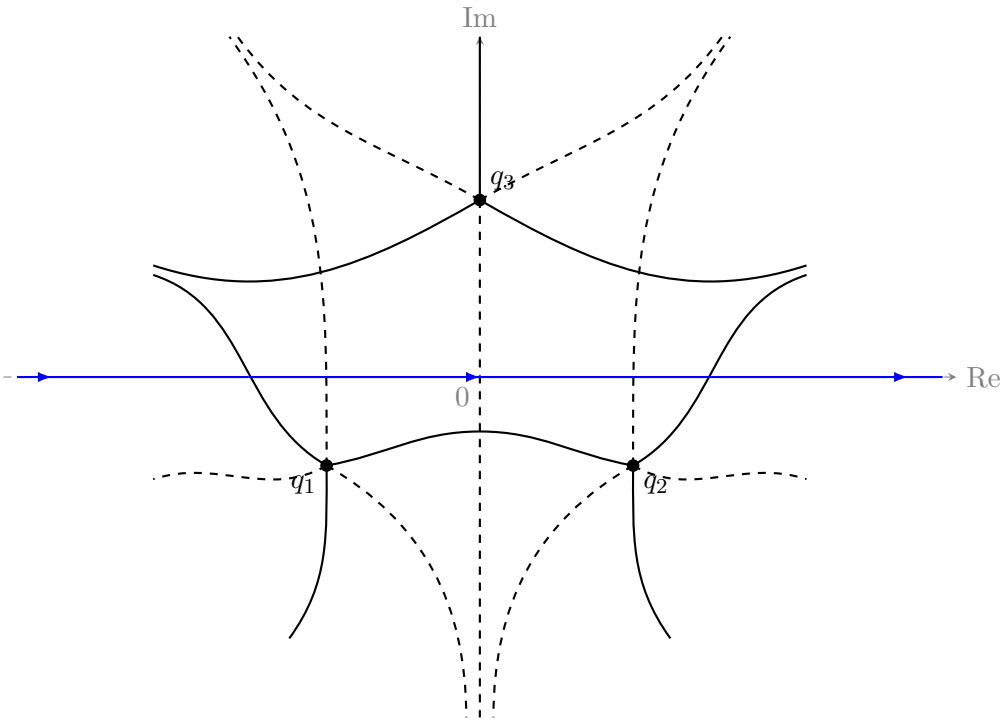


Figure 3.1: Sketch of the Stokes graph of iq^3 with solid anti-Stokes lines and dashed Stokes lines.

The anti-Stokes line that connects q_1 and q_2 shows that in zeroth order the quantization condition would be identical to the two turning point case, with the integral between q_1 and q_2.

For the full quantization condition the dominances of the solution, when we cross a Stokes line, need to be determined as well as the dominance in the asymptotic sectors of our contour. The dominance when crossing the Stokes lines needs to be with respect to its turning point. The dominant WKB solution has an exponent with a positive real part. Therefore we need to evaluate the

integral in equation (3.9) for values of q on our contour and analyse the real part. We need to evaluate the integral for all turning points as reference points. While doing so we need to stay on the same branch of the square root. This also includes checking that the path we choose, to integrate from the turning point to the real axis, remains on the same branch.

We find that for $q \to \pm\infty$, as well as at the Stokes line on the imaginary axis, ψ_+ is dominant. While we cross the Stokes lines of the turning points q_1 and q_2, ψ_- is dominant.

With the Stokes graph and the dominances we can construct the quantization condition for the approximated energy levels as seen above. We begin with the WKB solution at $q \to -\infty$ where ψ_+ is dominant, so our WKB solution only consists of $\psi = \psi_-$. The reference point we begin with is q_1. The first line crossed is an anti-Stokes line where ψ_- switches to dominant. At the Stokes line, which emerges from q_1, the coefficient of ψ_+ changes with $-i$ times the coefficient of ψ_-. Afterwards we need to change the reference point to q_3. This produces an exponential constant multiplied with the coefficient, which provides for ψ

$$\psi = \psi_- \to \psi = e^{-iS_{1,3}}\psi_- - ie^{iS_{1,3}}\psi_+ \tag{3.10}$$

$$\text{with} \quad S_{k,j} = \int_{q_k}^{q_j} \sqrt{E - V(q)}\mathrm{d}q. \tag{3.11}$$

Then we cross the next Stokes line and change the coefficient of ψ_- by adding the coefficient of ψ_+ multiplied with i because ψ_+ is dominant at q_3.

$$\psi = e^{-iS_{1,3}}\psi_- - ie^{iS_{1,3}}\psi_+ \to \psi = \left(e^{-iS_{1,3}} + e^{iS_{1,3}}\right)\psi_- - ie^{iS_{1,3}}\psi_+ \tag{3.12}$$

After that we need to change the reference point of the integral again to q_2 to use the connection condition at the third Stokes line. Doing this yields

$$\psi = \left(e^{-iS_{1,2}} + e^{-iS_{3,2}}e^{iS_{1,3}}\right)\psi_- - i\left(e^{iS_{1,2}} + e^{-iS_{1,2}} + e^{-iS_{3,2}}e^{iS_{1,3}}\right)\psi_+ \tag{3.13}$$

after the last Stokes line.

When moving further along to $q \to \infty$, we know that ψ_+ is dominant. Like seen above, the boundary condition of having normalizable states requires that the coefficient of ψ_+ is equal to zero. This gives us a condition in form of

$$2\cos\left(S_{1,2}\right) + e^{i(S_{1,3} - S_{3,2})} = 0, \tag{3.14}$$

which needs to hold and only depends on the energies.

The cos term is equal to the quantization condition with only two turning points, which was analyzed above. This term produces the known Sommerfeld quantization with a non-zero ground state energy. The second term describes tunnelling to the third turning point. The tunnelling is exponentially suppressed because the PT-symmetry of the turning points demands that $S_{1,3} - S_{3,2}$ is purely imaginary.

The quantization condition is solved by finding the roots of equation (3.14) with regards to the energies. The energies appear in the integrand of the actions $S_{j,k}$, as well as in the limits of the integral because of equation (3.4). The actions $S_{j,k}$, defined by the intergal in equation (3.11), can be calculated analytically by substituting $q = E^{1/3}x$. Then, the roots of the quantization condition can be found by known algorithms. The starting value given to the algorithm determines the energy level it converges to. The starting values can be taken from the numerical calculation of the energies, or one could neglect the exponential term and solve the condition analytically and use these values as starting values.

Solving the quantization condition and comparing the real parts of the solutions E_{WKB} to the real parts of the energies E_{exact}, found in the hermite basis, yields Tab. 3.1.

E_{exact}	E_{WKB}	$\frac{E_{exact}}{E_{WKB}}$	$E_{exact} - E_{WKB}$
1.1204	1.1563	1.0320	0.0359
4.0894	4.1092	1.0049	0.0199
7.5490	7.5623	1.0018	0.0133
11.3043	11.3144	1.0009	0.0102
15.2833	15.2916	1.0005	0.0083
19.4445	19.4515	1.0003	0.0071

Table 3.1: Energies calculated with the quantization condition and numerically by expansion in the hermite basis

As expected, the energies determined by the quantization condition improve for larger quantum numbers because of the WKB approximation. Nevertheless, even for the first states the quantization condition supplies energies that are within a few percent from the exact values.

The imaginary parts of both solutions compared are smaller than 10^{-6} and just results of the numerical calculation.

The WKB approximation also provides wavefunctions of the form of equation (2.9). We have already calculated the action S_0 from the turning points to the contour while analyzing the dominances of the solution. Also, while calculating the quantization condition, the wavefunction was modified when crossing a Stokes line. So in the different regions between the Stokes lines, the wavefunction will have a different form.

From $q \to -\infty$ until the first Stokes line the wavefunction ψ is just given by

$$\psi = \frac{C}{\sqrt{p(q)}} e^{-iS_1(q)}, \tag{3.15}$$

$$\text{with } S_m = \int_{q_m}^{q} \sqrt{E - V(\tilde{q})}\mathrm{d}\tilde{q}, \tag{3.16}$$

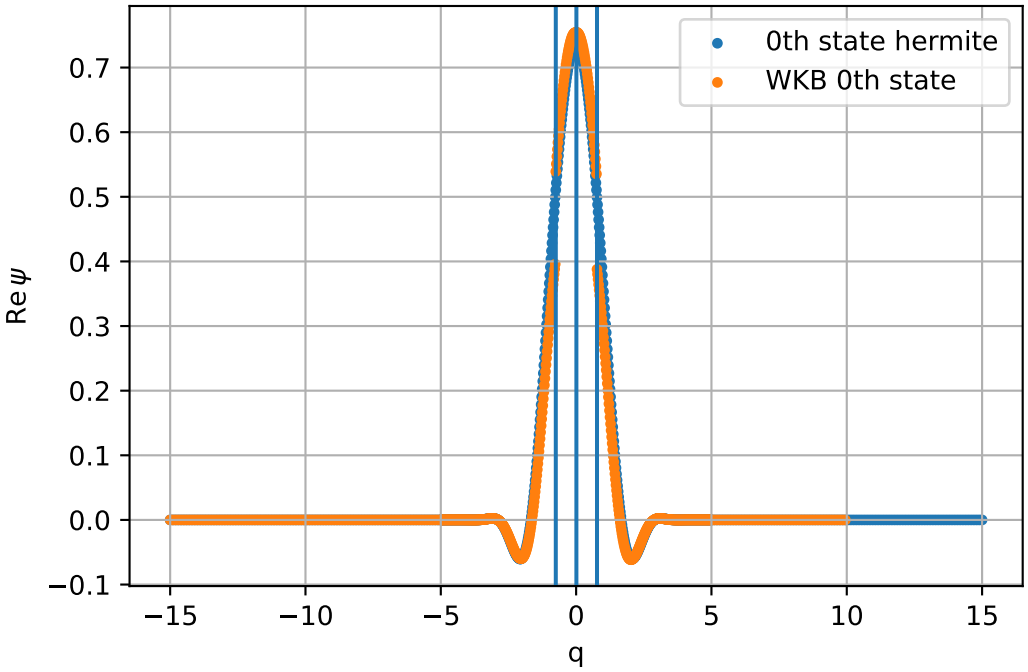


Figure 3.2: Ground state for $\alpha = 0$ with WKB approximation and the crossing of the Stokes lines

where C is a constant to normalize the wavefunction. Between the first and second Stokes line

$$\psi = \frac{C}{\sqrt{p(q)}} \left[e^{-iS_1(q)} - ie^{iS_1(q)} \right]. \tag{3.17}$$

After passing the second Stokes line, the wavefunction becomes

$$\psi = \frac{C}{\sqrt{p(q)}} \left[(1 + e^{2iS_{1,3}}) e^{-iS_1(q)} - ie^{iS_1(q)} \right]. \tag{3.18}$$

After the third Stokes line, the ψ_+ part of the solution is not normalizable, so the approximated wavefunction just consists of the ψ_- part. This means for the section from the third Stokes line until $q \to \infty$

$$\psi = \frac{C}{\sqrt{p(q)}} (1 + e^{2iS_{1,3}}) e^{-iS_1(q)}. \tag{3.19}$$

Comparing the WKB wavefunctions with the wavefunctions obtained in Sec. 3.1 shows that besides the energies, also the wavefunctions are well approximated. The comparison for the ground states and first excited states is shown in Fig. 3.2 and Fig. 3.3.

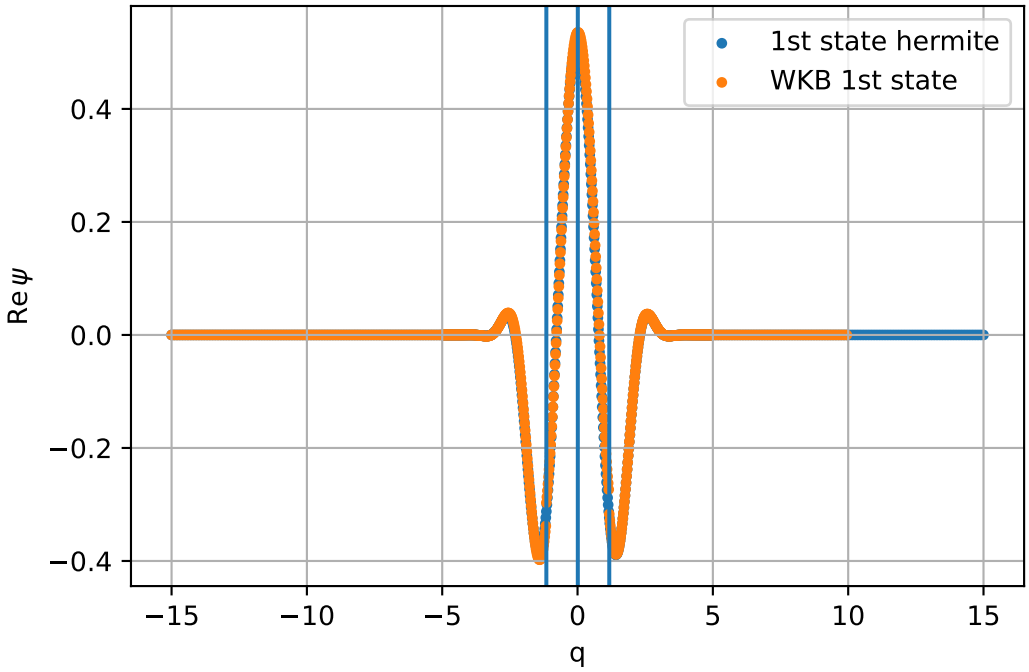


Figure 3.3: First excited state for $\alpha = 0$ with WKB approximation and the crossing of the Stokes lines

3.2.2 PT-symmetry breaking for $\alpha < 0$

The potential iq^3 is now modified by a linear term $i\alpha q$, with a real parameter α.

Because the structure of the Stokes graph should depend continuously on α, for α near zero, the general structure of the Stokes graph should remain the same. This means the quantization condition will have the same form, at least for some α near zero. The evaluation of the quantization condition will differ because the actions, as well as the turning points, now involve an extra term. The turning points, as roots of a third degree polynomial, can still be calculated analytically. The integral defining the actions can be traced back to a complete elliptic integral. Both quantities can also be calculated numerically.

The spectrum should also depend continuously on α. Therefore, to find the spectrum for any α, the energies can be calculated iteratively by starting at $\alpha = 0$ and increasing α in steps until the wanted value. In each step the previous values of the energies can be used as initial values.

Increasing α from zero shows that for all positive α, the spectrum is completely real. This is again verified by the spectra calculated numerically by expanding the states in the hermite basis. With the energies, we can now look at the turning points for the ground state energy in Fig. 3.4. With the asymp-

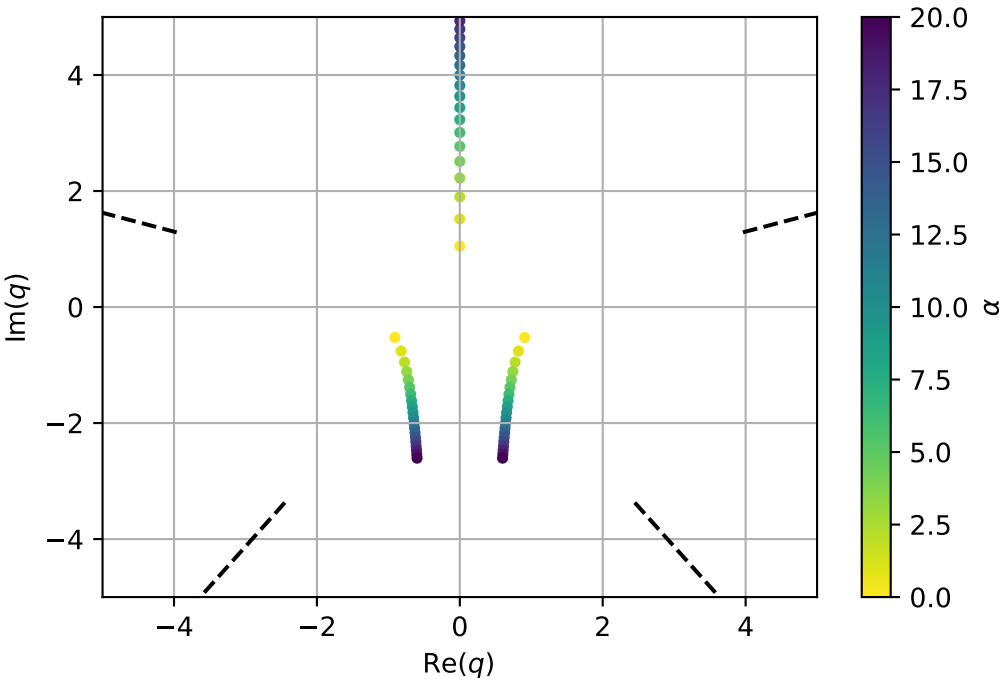


Figure 3.4: Turning points for increasing α with asymptotic anti-Stokes lines

totic anti-Stokes lines, this verifies that the structure of the Stokes graph is preserved. Additionally, the purely imaginary exponent in the quantization condition (3.14) becomes large, so that the influence of the third turning point vanishes exponentially.

The same procedure for negative α shows that at some $\alpha_c(0)$, the quantization condition does not converge for the ground state energy. Adding an imaginary part to the initial values from the beginning solves this problem. Then the quantization condition yields complex conjugated pairs of energies for the ground state and first excited state. When α decreases, this effect appears for the next two states at $\alpha_c(1)$ and so on. The exact numerically determined energies back these results. In general for $\alpha < \alpha_c(n)$ the $2n$-th and $2n+1$th excited states break PT-symmetry and we have a pair of complex conjugated energies.

For negative α, the exponent in the quantization condition increases, which can be interpreted as a more probable tunnelling of the particle to the third turning point. At some α, $\left|e^{i(S_{1,3}-S_{3,2})}\right| > 2$ and $S_{1,2}$ needs to be complex to solve the condition. This requires that q_1 and q_2 are not PT-symmetric to each other because the integral would be real.

Again, the turning points and the Stokes graph can be analyzed after obtaining the energies. The turning points have the same structure until the PT-symmetry is broken. Then q_1 and q_2 are no longer PT-symmetric to each other, but if q_n is a turning point to E then $\mathcal{PT}q_n$ is a turning point to E^*.

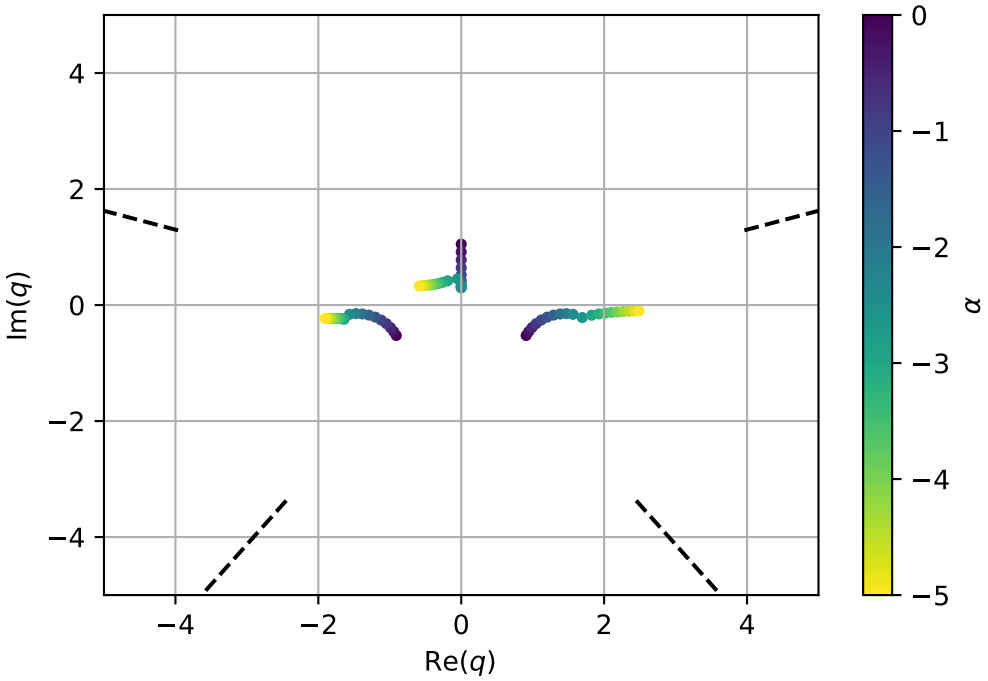


Figure 3.5: Turning points for decreasing α and $\mathrm{Im}\, E > 0$ with asymptotic anti-Stokes lines

Also the turning point q_3 leaves the imaginary axis. The behavior can be seen in Fig. 3.5.

Moreover, the structure of the anti-Stokes lines changes for $\alpha < 0$. For an $\alpha > \alpha_c$ but smaller than 0, the anti-Stokes line connecting q_1 and q_2 now passes through q_3. Afterwards there is no connection between the turning points, as all anti-Stokes lines approach ∞ seen in A. This behavior can be tracked by solving

$$\mathrm{Re}\, i \int_{q_n}^{q} \sqrt{E - V(\tilde{q})} \mathrm{d}\tilde{q} = 0 \tag{3.20}$$

which yields where the anti-Stokes lines cross the real axis.

While α is further decreasing, the turning point q_3 is getting closer to q_1 and the influence of the turning point q_2 is shrinking. The quantization condition can be multiplied by $e^{-iS_{2,3}}$ to rewrite it as

$$2cos(S_{1,3}) + e^{i(S_{1,2} - S_{2,3})} = 0, \tag{3.21}$$

which is a more suitable form for this regime of α. The second term becomes exponentially small, so that the anti-Stokes lines emerging from q_1 and q_3 get closer. If the term is neglected, q_1 will be connected to q_3 again and the Stokes graph has the form of Fig. 3.6.

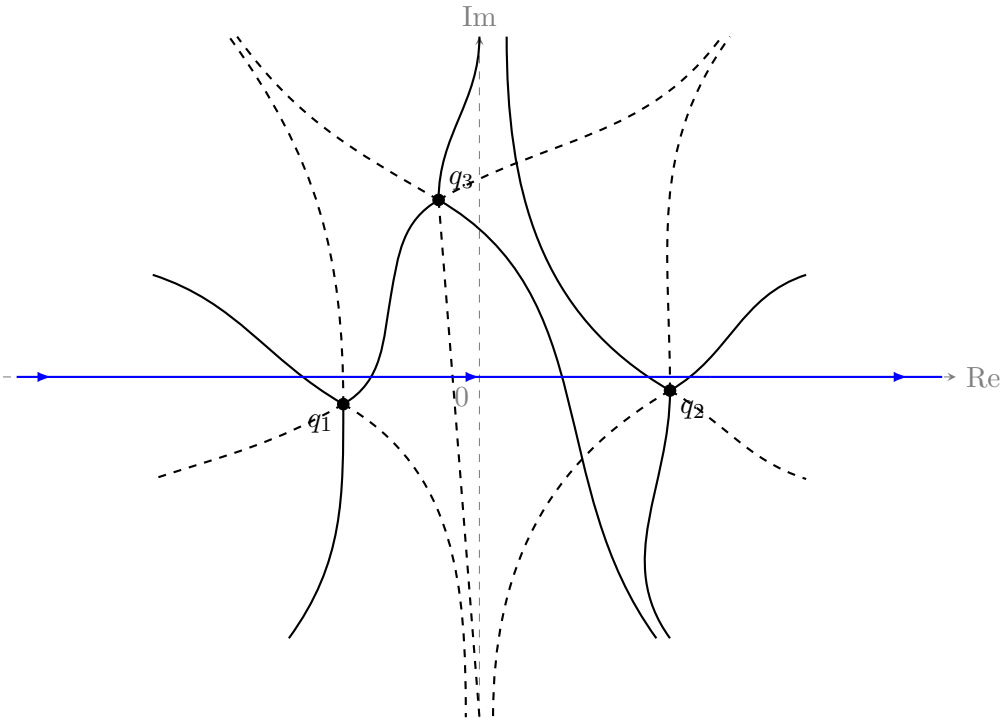


Figure 3.6: Sketch of the Stokes graph of iq^3 with solid anti-Stokes lines and dashed Stokes lines for $\alpha < \alpha_c$

To determine the $\alpha_c(n)$ for the PT-symmetry breaking of all pairs of states ψ_{2n} and ψ_{2n+1}, we will use two methods.

The first method is based on fitting the behavior of $E(\alpha)$ near α_c to calculated energies for different α. The fit provides α_c as a fitting parameter.

The local behavior of E near α_c can be obtained by reducing $H = H_0 + H_1$, where $H_0 = p^2 + iq^3$ and $H_1 = i\alpha q$, to the effective Hamilton operator H_{eff} with

$$H_{eff} = \begin{pmatrix} \langle 0| H |0\rangle & \langle 0| H |1\rangle \\ \langle 1| H |0\rangle & \langle 1| H |1\rangle \end{pmatrix} \tag{3.22}$$

$|0\rangle$ and $|1\rangle$ are eigenstates of H_0. We only need to calculate $\langle i| H_1 |j\rangle$ because H_0 will add just the real eigenvalues ε_0 or ε_1. The inner product is given by $\langle i \mid j\rangle = \int \psi_i \psi_j \mathrm{d}q$. With the PT-symmetry of the states ψ_j, it is straightforward to show that all integrals and so the matrix elements are real. With $\langle \psi_j \mid \psi_j\rangle = (-1)^j$ we obtain

$$\begin{pmatrix} \varepsilon_0 + \alpha a & \alpha b \\ \alpha b & -\varepsilon_1 + \alpha c \end{pmatrix} \tag{3.23}$$

where a,b,c are real constants. With $a(\alpha) = \varepsilon_0 + \alpha a$ and $c(\alpha) = -\varepsilon_1 + \alpha c$, the effective Hamilton operator yields the energies

$$E_\pm = \frac{a(\alpha) - c(\alpha)}{2} \pm \frac{1}{2}\sqrt{(a(\alpha) + c(\alpha))^2 - 4\alpha^2 b^2}. \tag{3.24}$$

At $\alpha = \alpha_c$ the energies of the two states become equal $E_+ = E_- = E_c$, so that the expression under the square root needs to be zero. The behavior of E_+ and E_- describes the behavior of all E_n and E_{n+1} near $\alpha_c(n)$. The already calculated energies $E_n(\alpha)$ and $E_{n+1}(\alpha)$ are subtracted and squared, so that we can fit $d(\alpha-\alpha_c)+e(\alpha-\alpha_c)^2$ to $(E_{n+1}(\alpha)-E_n(\alpha))^2$. The real parameters d, e, and α_c are results of the fit. Examples of the fit can be found in appendix A.

The second method utilizes the condition for a double root. At $\alpha = \alpha_c(n)$ and $E_n = E_{n+1} = E_c$, the quantization condition is equal to zero, as well as its derivative because of the double root. We introduce U and V, with $U+iV = S_{1,2}$ and U,$V \in \mathbb{R}$. Due to the PT-symmetry in the unbroken region of α, we can write the quantization condition as $2cos(2U)+e^{-2V} = 0$. Before calculating the $\alpha_c(n)$, we set $\alpha \to -\alpha$ because we already know we are interested in negative α.

The condition for the double root at $\alpha_c(n)$ yields the equations

$$cos(2U) = -\frac{1}{2}e^{-2V} \tag{3.25}$$

$$\text{and} \quad sin(2U) = -\frac{1}{2}\frac{V'}{U'}e^{-2V}. \tag{3.26}$$

These equations bound V for large α_c and E_c because otherwise the right side of both equations would be zero and the equations would not have any solutions.

Now we rescale our potential with $q \to \sqrt{\alpha}q$, which supplies

$$U + iV = \alpha^{5/4}\int_{q_1}^{q_2}\sqrt{\varepsilon - iq^3 + iq}\mathrm{d}q. \tag{3.27}$$

q_1, q_2, and q_3 are now the solutions of the equation $q^3 - q + i\varepsilon = 0$ and $\varepsilon = E\alpha^{-3/2}$. We define $\tilde{U} + i\tilde{V} = (U + iV)\alpha^{-5/4}$. For $\alpha_c \to \infty$ and $E_c \to \infty$, V is bounded, which means $\tilde{V} = V\alpha^{-5/4}$ goes to zero. This defines an ε_∞ by

$$\int_{q_1}^{q_2}\sqrt{\varepsilon_\infty - iq^3 + iq}\mathrm{d}q = 0, \tag{3.28}$$

which can be used to expand and approximate all ε_n in the rescaled quantization condition and so $\alpha_c(n)$. This approximation is good for large α_c and E_c, but as we will see is sufficient even for the lowest states.

We will include the first-order perturbation of ε_n in $1/\lambda_n = \alpha_c(n)^{-5/4}$ to improve the result for the smaller $\alpha_c(n)$. In first-order, $\varepsilon_n = \varepsilon_\infty + \delta/\lambda_n$.

Furthermore, $\tilde{V}(\varepsilon_n) \approx \tilde{V}(\varepsilon_\infty) + \tilde{V}'(\varepsilon_\infty)\delta/\lambda_n = \tilde{V}'(\varepsilon_\infty)\delta/\lambda_n$, as well as $\tilde{U}(\varepsilon_n) \approx \tilde{U}(\varepsilon_\infty) + \tilde{U}'(\varepsilon_\infty)\delta/\lambda_n$. Respecting the right branch, the quantization condition can be written as

$$2U(\varepsilon_n) = 2\pi(n+1) - \arccos\left[-\frac{1}{2}e^{-2V(\varepsilon_n)}\right]. \tag{3.29}$$

For $U(\varepsilon_n)$ and $V(\varepsilon_n)$ we can substitute $\tilde{U}(\varepsilon_n)\lambda_n$ and $\tilde{V}(\varepsilon_n)\lambda_n$ and use the expansion in $1/\lambda_n$, which yields

$$2\lambda_n \left[\tilde{U}(\varepsilon_\infty) + \frac{\delta}{\lambda_n}\tilde{U}'(\varepsilon_\infty)\right] = 2\pi(n+1) - \arccos\left[-\frac{1}{2}e^{-2\delta\tilde{V}'(\varepsilon_\infty)}\right]. \tag{3.30}$$

The only term still unknown is δ. Squaring and adding equations (3.25) and (3.26) provides $1/2e^{-2V} = (1 + V'^2/U'^2)^{-1/2}$. Using $V/U = \tilde{V}/\tilde{U}$ and taking only orders independent of λ into account, because orders of $1/\lambda$ would supply orders of $1/\lambda^2$ in ε_n, the expression can be solved for δ with

$$\delta = -\frac{1}{2\tilde{V}'(\varepsilon_\infty)} \ln\left[2\left(1 + \frac{\tilde{V}'^2(\varepsilon_\infty)}{\tilde{U}'^2(\varepsilon_\infty)}\right)^{-\frac{1}{2}}\right]. \tag{3.31}$$

This brings equation(3.30) to

$$\begin{aligned}\lambda_n =& \frac{1}{2\tilde{U}(\varepsilon_\infty)}\Bigg\{2\pi(n+1) - \arccos\left[-\left(1 + \frac{\tilde{V}'^2(\varepsilon_\infty)}{\tilde{U}'^2(\varepsilon_\infty)}\right)^{-\frac{1}{2}}\right] \\ &+ \frac{\tilde{U}'(\varepsilon_\infty)}{\tilde{V}'(\varepsilon_\infty)} \ln\left[2\left(1 + \frac{\tilde{V}'^2(\varepsilon_\infty)}{\tilde{U}'^2(\varepsilon_\infty)}\right)^{-\frac{1}{2}}\right]\Bigg\}.\end{aligned} \tag{3.32}$$

Equation (3.32), with $\alpha_c(n) = \lambda_n^{4/5}$, yields all $\alpha_c(n)$ where the PT-symmetry of the $2n$-th state and $2n+1$-th state is broken and the energies become complex conjugated pairs.

To calculate the $\alpha_c(n)$, we use the analytical expressions for the turning points q_j of the rescaled potential

$$q_j = 2\sqrt{\frac{1}{3}} \cos\left[\frac{1}{3}\arccos\left(-\frac{3i\varepsilon\sqrt{3}}{2}\right) - \frac{2\pi(j-1)}{3}\right] \tag{3.33}$$

and for $\tilde{V}$,$\tilde{U}$, we trace the integral back to a complete elliptic integral. The derivatives can then be obtained by known rules.

Both methods can provide $\alpha_c(n)$ for all n. The α_c of the first states are compared in Tab. 3.2, where we can see that despite the approximation in the second approach, the deviation lies within the underlying error of the WKB approximation. For further calculations we will prefer the second method because of the simplicity and efficiency.

We can also determine the wavefunctions equivalently to the unbroken case. Because of the PT-symmetry breaking, the states with a complex conjugated pair of energy have wavefunctions which fulfill $\psi_n = \mathcal{PT}\psi_{n+1}$. The wavefunctions for a pair of these states can be seen in appendix A.

n	$\alpha_c(n)$ from fit to E_{exact}	$\alpha_c(n)$ from fit to E_{WKB}	$\alpha_c(n)$ by expanding ε
0	-2.622	-2.589	-2.613
1	-5.376	-5.368	-5.388
2	-7.813	-7.810	-7.830
3	-10.073	-10.071	-10.090

Table 3.2: Comparison of $\alpha_c(n)$ for the different methods

3.3 Potential $-iq^5 + i\alpha q$

The potential $-iq^5 + i\alpha q$ will have similarities to the potential $iq^3 + i\alpha q$, which will demonstrate some patterns for these kinds of potentials. At the same time the potential provides new insights, which can also be applied to other problems.

3.3.1 Spectrum for two pairs of turning points

Again, we will start with α set to zero and consider the energies to be real for this case. The turning points and the Stokes graph are determined analogously to the potential iq^3. Because of the higher exponent, the potential will have 5 turning points and the Stokes- and anti-Stokes lines will asymptotically approach seven different angles. At each turning point, three Stokes- and anti-Stokes lines will emerge. Considering the PT-symmetry, the Stokes graph is sketched in Fig. 3.7.

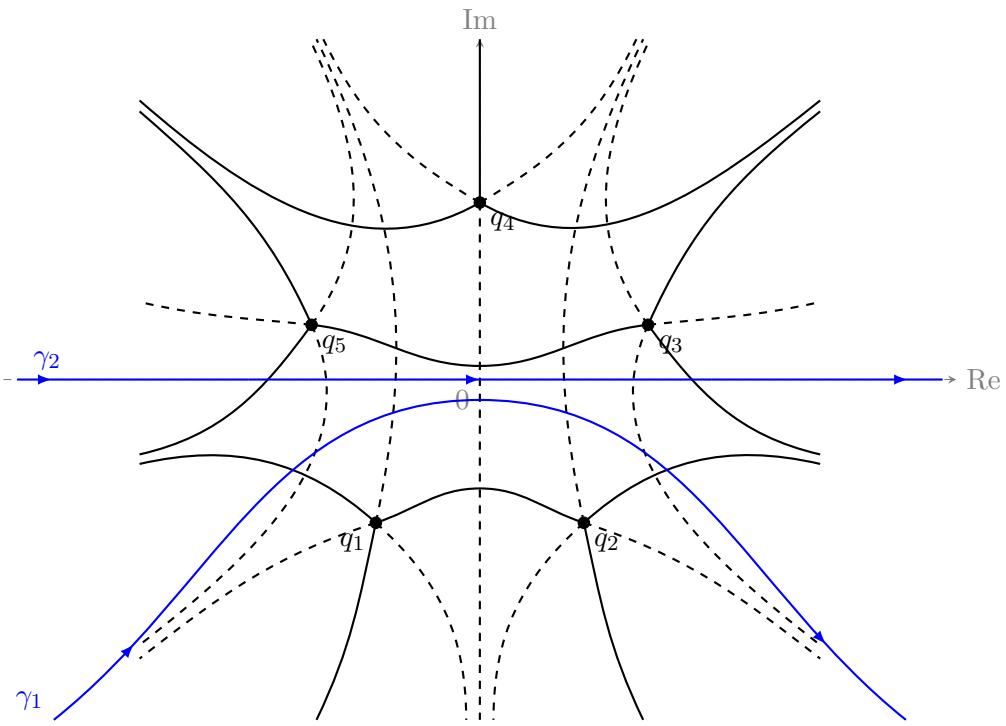


Figure 3.7: Sketch of the Stokes graph of iq^5 with solid anti-Stokes lines and dashed Stokes lines.

Before calculating the spectrum, we need to impose a boundary condition to our wavefunctions. If we want to consider the boundary condition inside the same Stokes sector as for the potential $V(q) = iq^3$, we can not choose the real axis anymore. The asymptotic Stokes sectors rotate when the exponent of the potential is smoothly increased [8]. The sectors, in which the contour did lie for $V(q) = iq^3$, are rotated downwards into the complex plane. Therefore we can either choose wavefunctions that are normalizable on a contour of the form γ_1 seen in Fig. 3.7, or on the real axis with γ_2. The first choice would be the smoothly adjusted problem from the potential iq^3.

We will first analyze the spectrum with normalizable states on the contour γ_1. Just as above, we need to determine which part of the WKB solution is dominant at the crossing of the 5 Stokes lines, as well as which solution is dominant for $|q| \to \infty$. This is again done by integrating $p(q)$ from the turning points to the contour while taking the branch cuts into account. Asymptotically and at the Stokes lines emerging from q_3, q_4, and q_5, ψ_+ is the dominant part of the WKB solution. Only at the Stokes lines of q_1 and q_2, ψ_- is dominant.

Because the Stokes lines emerging from q_5 and q_3 are the first and last Stokes lines crossed, while having the same dominance as asymptotically, these turning points do not contribute to the quantization condition. This means the process of connecting the solution across the Stokes lines and demanding normalizable states yields

$$2\cos(S_{1,2}) + e^{i(S_{1,4}-S_{4,2})} = 0. \tag{3.34}$$

The quantization condition has the same form as for the potential $V(q) = iq^3$ in the same, rotated sector.

To calculate the energies numerically by the expansion in the hermite basis, we need to substitute q in the Hamilton operator. To describe the problem on the contour, we plug in the parametrization $q = x - i\sqrt{(\tan 3\pi x/14)^2 + 0.2}$ before beginning the calculation. The real parameter x is then expressed by the ladder operators. Of course we need to substitute p as the derivative as well. Then, we can calculate the spectrum again as eigenvalues of the $N \times N$ matrix. Comparing the energies with the ones provided by the quantization condition yields Tab. 3.3, which shows again the strength of the WKB approximation.

E_{exact}	E_{WKB}
1.908	1.778
8.587	8.509
17.711	17.653
28.595	28.547

Table 3.3: Numerically calculated and WKB approximated energies for the contour γ_1

Regarding the contour on the real axis, the dominances at the crossings of the Stokes lines are identical to the dominances at the crossings of the contour in the lower half-plane. This should not be surprising because the Stokes lines cross

both contours without an anti-Stokes line in between, where the dominances would change. The dominance in the asymptotic sector, however, is different, and for the real axis, ψ_- is the dominant solution for $|q| \to \infty$. Following the procedure for the connection at the Stokes lines yields

$$\begin{aligned} &2\cos(S_{5,3}) + e^{i(S_{5,4}-S_{4,3})} + e^{-i(S_{5,1}-S_{1,3})} + e^{-i(S_{5,2}-S_{2,3})} \\ &+ e^{i(S_{5,3}-2S_{4,2})} + e^{-i(S_{5,3}-2S_{1,4})} + e^{i(S_{5,4}-S_{4,3})+2i(S_{1,4}-S_{4,2})} = 0 \end{aligned} \tag{3.35}$$

as the quantization condition. Here all turning points influence the condition. On the real axis we can again verify the energies with the purely numerical calculation.

3.3.2 PT-symmetry breaking

We now again analyze the potential for $\alpha \neq 0$.

The quantization condition for the contour in the complex plane is the same as for the potential iq^3, so that the PT-symmetry breaking will again occur for negative α. The Stokes graph will again change in such a manner that the anti-Stokes line between q_1 and q_2 is broken. Then the anti-Stokes line of q_4 will get close to the one from q_1, and for $\alpha \to -\infty$ the anti-Stokes lines will be connected. Also the $\alpha_c(n)$ can be determined analogously by utilizing the condition for the double root of the quantization condition and rescaling the potential.

An effect, which can not yet be explained, is that for decreasing α, the energies turn negative before becoming complex. The quantization condition can not provide these negative, real energies but is converging to another energy level. As soon as the energies become complex, the quantization condition again converges to the complex energy.

With the boundary condition on the real axis, we need to analyze the case for $\alpha \neq 0$ more carefully. The different quantization condition will provide a different behavior when α is changing from zero. First, for negative α, the PT-symmetry is again broken. This starts at the ground state similar to the already analyzed cases. When comparing the actions between the turning points and the different exponential terms in (3.35) for α near α_c, only one exponential term contributes substantially to the condition besides the cos term. Near α_c the quantization condition can be reduced to

$$cos(S_{5,3}) + e^{i(S_{5,4}-S_{4,3})} = 0. \tag{3.36}$$

Again the effective quantization condition has the same form. Only the turning point, which is located on the imaginary axis for $\alpha > \alpha_c$, and the two turning points in the Stokes sector, in which the contour lies, contribute, and the α_c can be determined. The change in the Stokes graph is also equivalent to the breaking analyzed above.

For the boundary condition on the real axis, increasing α from zero also produces PT-symmetry breaking. Again comparing the actions and the exponential terms yields that all terms can be neglected besides the cos term and the

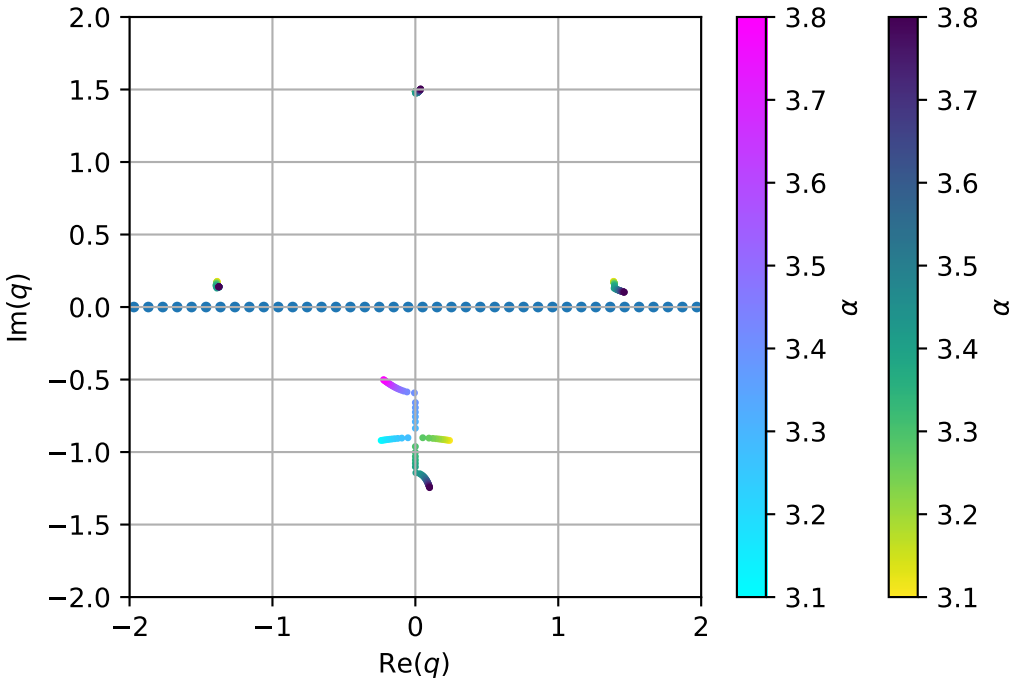


Figure 3.8: Turning points for positive α around the PT-symmetry breaking of the ground state

exponential terms including $S_{5,1}$ and $S_{5,2}$. This provides the simpler condition for α near α_c

$$cos(S_{5,3}) + e^{-i(S_{5,1}-S_{1,3})} + e^{-i(S_{5,2}-S_{2,3})} = 0 \tag{3.37}$$

So for positive α, the tunneling to the turning points in the lower half-plane increases, and those are responsible for the PT-symmetry breaking. Before the actual breaking, the turning points q_1 and q_2 move together onto the real axis and then away from each other until the symmetry breaks, like seen in Fig. 3.8. The Stokes graph changes similar to above, so that the turning point q_5 is nearly connected to turning point q_1 by an anti-Stokes line after the PT-symmetry breaking.

Going further, the turning point q_1 is the relevant turning point for the PT-symmetry breaking. Comparing the kept exponential terms in terms of magnitude shows that the tunneling to q_2 is not negligible but smaller than to q_1. To calculate the α_c, we can reduce the quantization condition even more by erasing the second term in equation (3.37). This produces energies that differ more from the numerically exact determined energies but provides the same α_c. With the quantization condition reduced to one exponential term, we can again use the derived formalism in Sec. 3.2.2 to calculate all $\alpha_c(n)$. These match again with estimated α_c we get from calculating the energies for different α around the point where the energies turn complex.

The PT-symmetry breaking and therefore the determination of the $\alpha_c(n)$ can in all analyzed cases be reduced to three turning points and to the simple quantization condition. This works for a PT-invariant turning point on the imaginary axis, as well as for a pair of turning points which first move onto the axis.

Chapter 4

Conclusion and outlook

In this thesis we analyzed PT-symmetric Hamiltonians and have shown that the WKB approximation is a powerful tool to get deeper insight into the PT-symmetry breaking. By using the presented formalism with the WKB approximation, a quantization condition was constructed that includes contributions from all turning points that are important for the problem. We have seen that the obtained quantization condition provides good energy levels, even for the lowest states. While modifying the potential with the parameter α, the condition stays valid, and the exponentially small tunneling terms become significant, as the pair of relevant turning points switches.

Subsequently, it was shown that the PT-symmetry breaking, for changing α, begins at the lowest states because these more localized states are more strongly affected by the change in potential. For all potentials a third turning point, besides the pair of turning points in the same Stokes sector as the boundary condition, was sufficient to describe the PT-symmetry breaking. With the reduction to the three turning points, a formula for the determination of all $\alpha_c(n)$ was derived that could reliably produce the right α.

Building on this work, there are some ways to extend our knowledge about these potentials and the PT-symmetry breaking further. First, one could investigate what properties a turning point, or pair of turning points, must have to be included in the PT-symmetry breaking. In the symmetry breaking of the states of the potential $-iq^5+i\alpha q$, with the boundary condition in the lower half-plane, only the turning point q_4 on the imaginary axis was included. The turning points q_3 and q_5 had no impact. Potentials with even more turning points could have different structures for the PT-symmetry breaking. One could investigate if the reduction to a three turning point problem is still valid.

Another approach, with a similar aim, would concern the deformation itself. Both analyzed potentials were modified by the same linear term. PT-symmetry covers a larger class of deformations. It could be determined which class of deformations breaks the PT-symmetry and which leaves the spectrum real. The results of our work suggest that the PT-symmetry is broken as soon as the

tunneling term can not be compensated by a real action between the turning points in the sector. This would hold for any deformation and also solve the question above.

Lastly, the mentioned negative energies and the failure of the quantization condition to provide these energies, for negative α and the potential $-iq^5 + i\alpha q$, could be of interest. It has to be mentioned that it is possible that this effect results simply from poor managing of the branches but could not yet be solved.

Appendix A

Additional figures

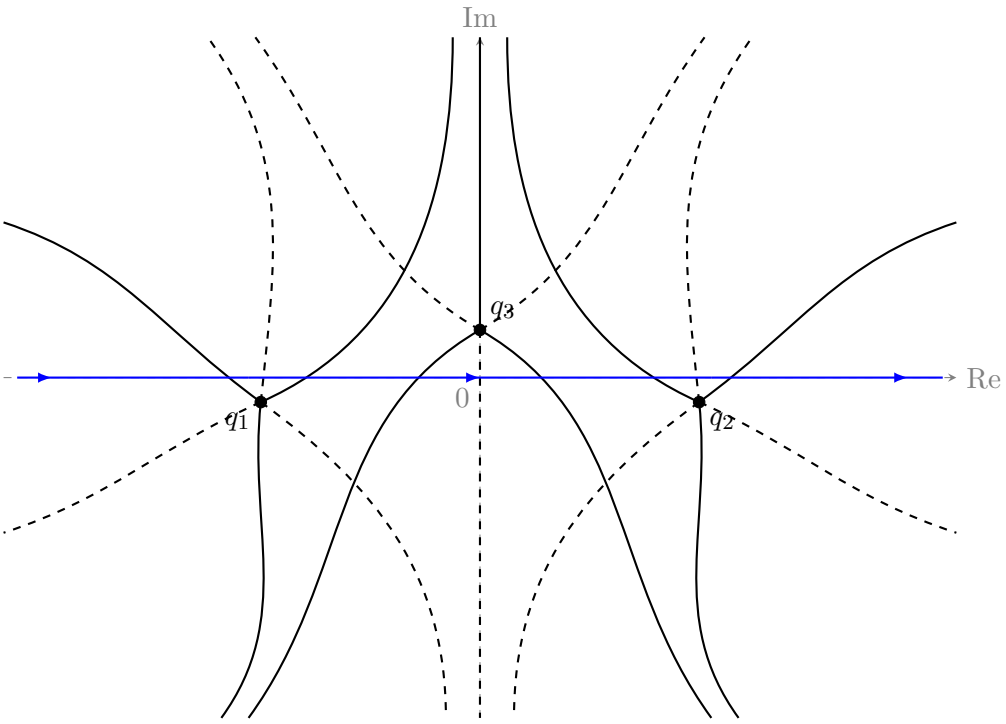


Figure A.1: Sketch of the Stokes graph of $iq^3 + i\alpha q$ at $\alpha = -2.5 > \alpha_c$ with solid anti-Stokes lines and dashed Stokes lines.

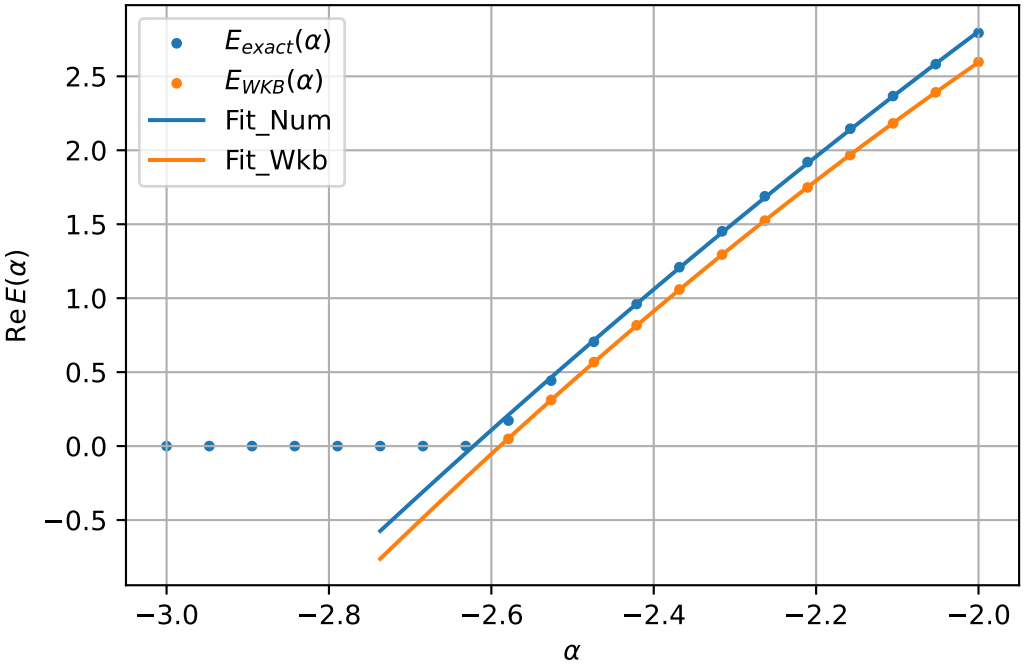


Figure A.2: Fit to $E_1(\alpha)^2 - E_0(\alpha)^2$ to determine $\alpha_c(0)$

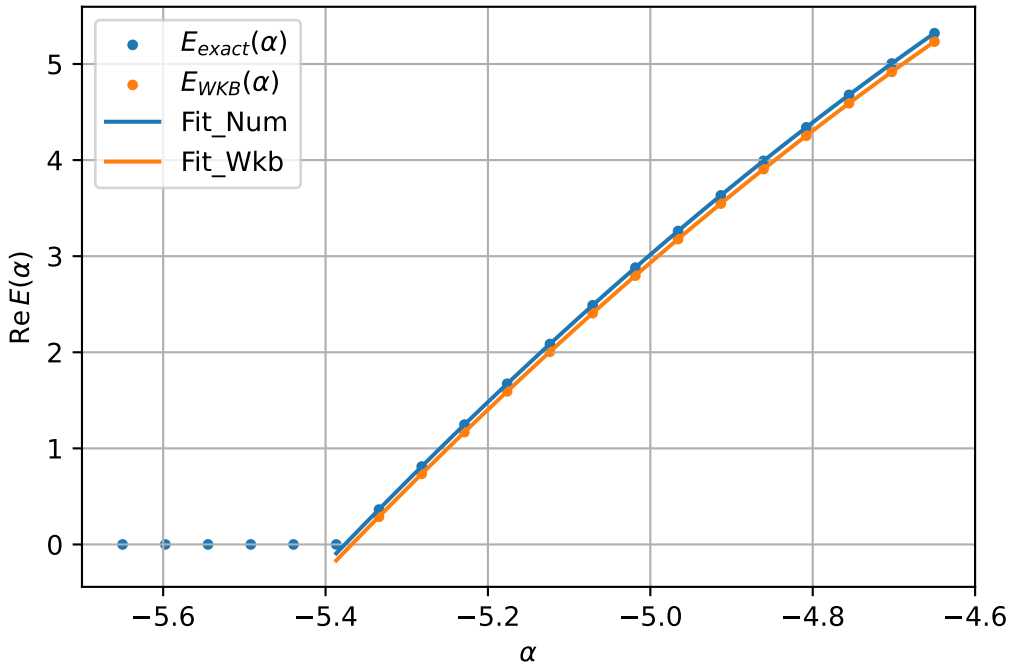


Figure A.3: Fit to $E_3(\alpha)^2 - E_2(\alpha)^2$ to determine $\alpha_c(1)$

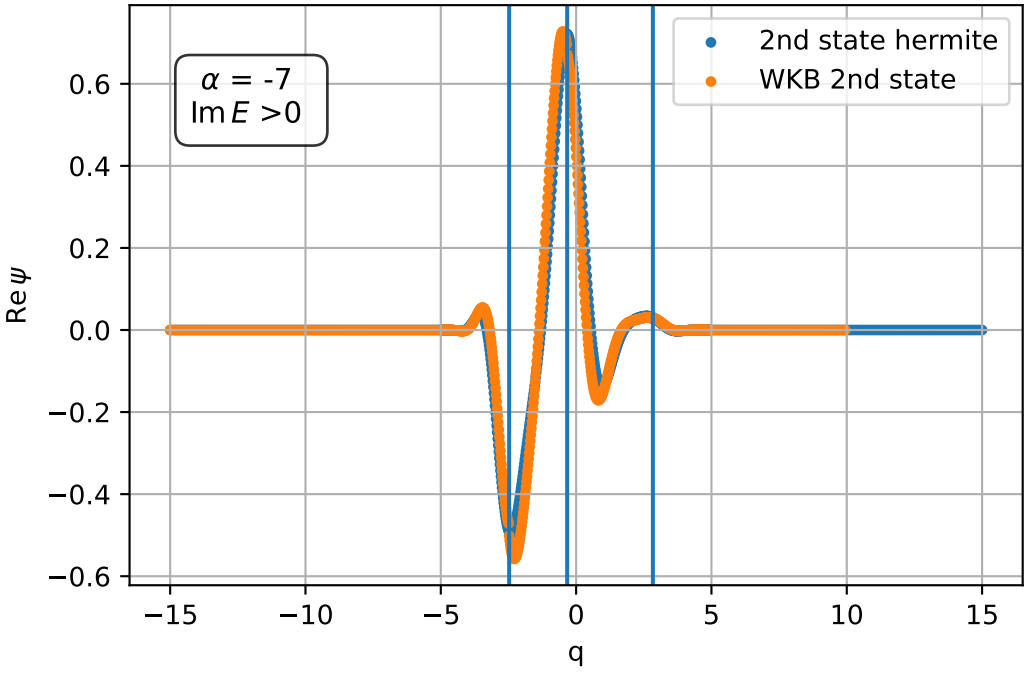


Figure A.4: Real part of ψ_2 for $\alpha < \alpha_c(1)$

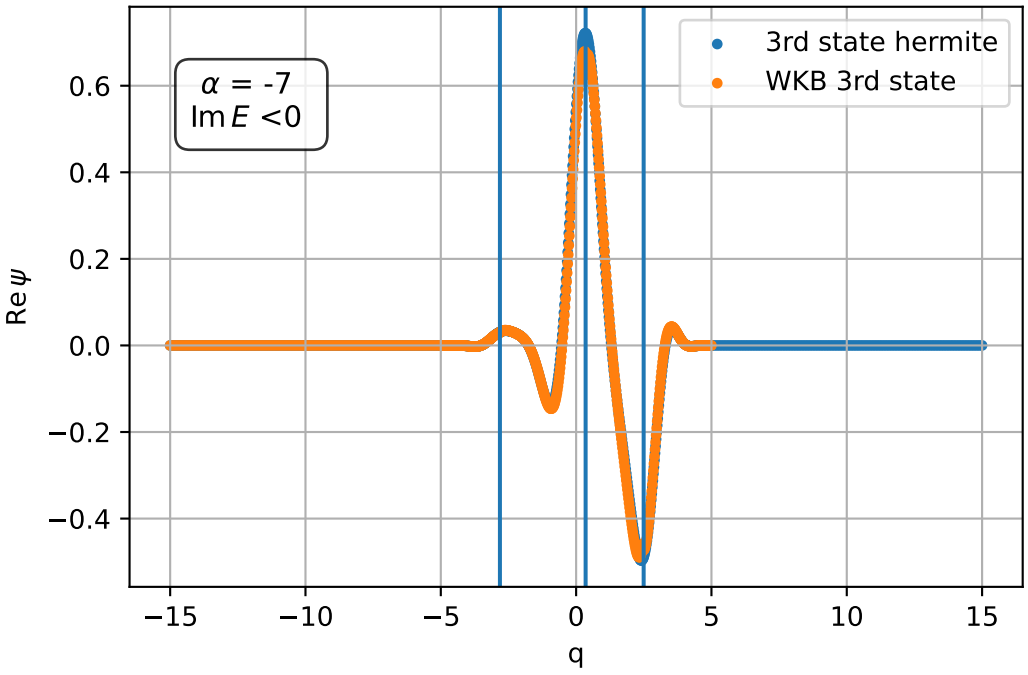


Figure A.5: Real part of ψ_3 for $\alpha < \alpha_c(1)$

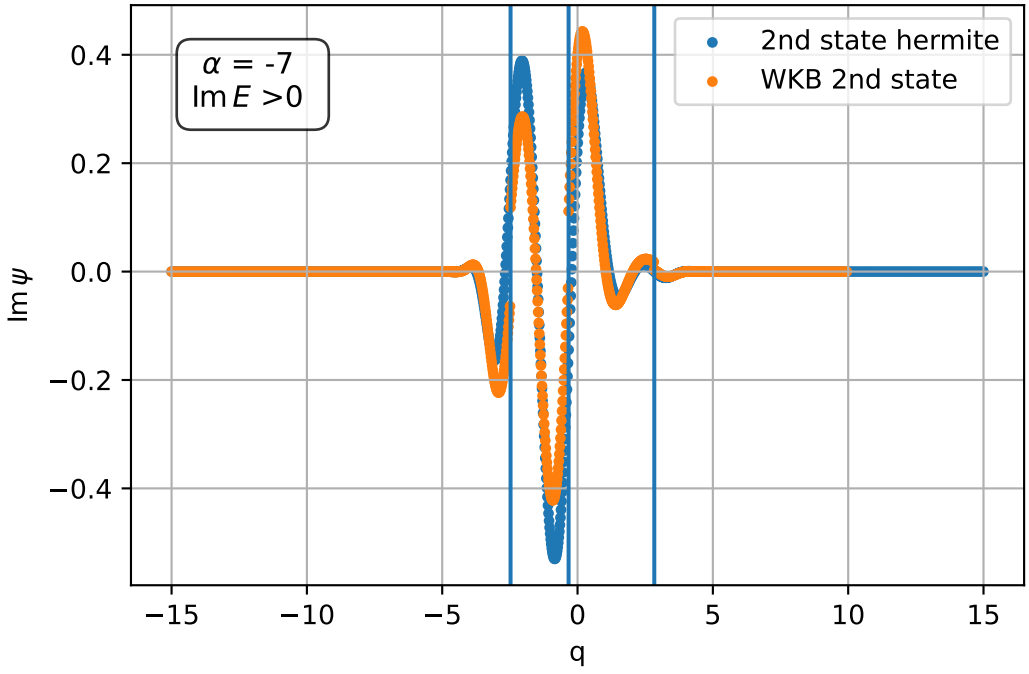


Figure A.6: Imaginary part of ψ_2 for $\alpha < \alpha_c(1)$

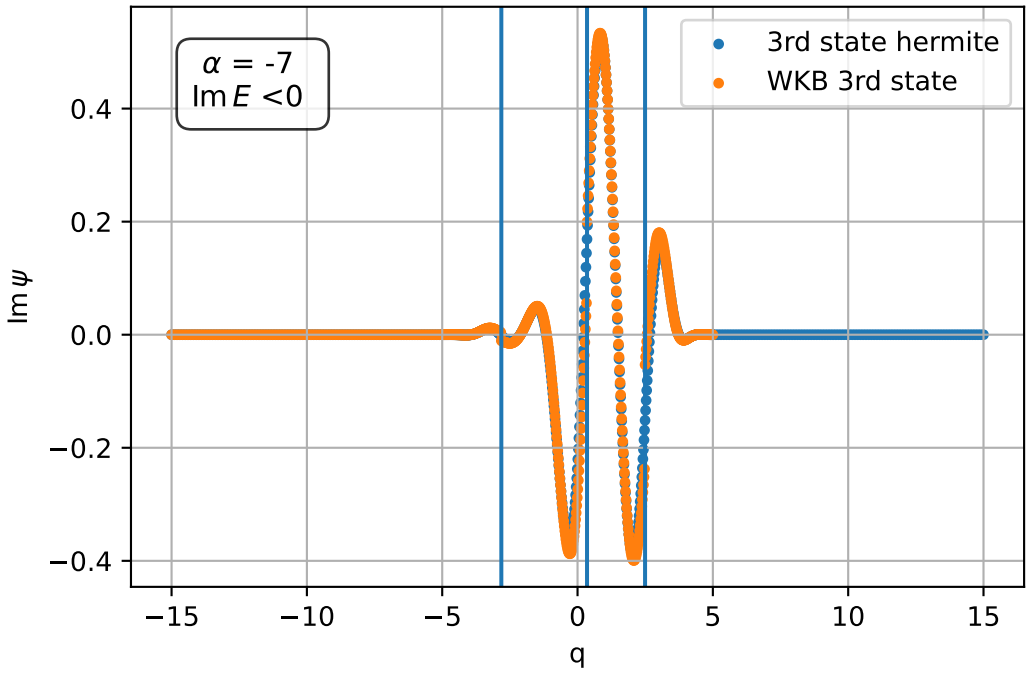


Figure A.7: Imaginary part of ψ_3 for $\alpha < \alpha_c(1)$

Bibliography

[1] Carl M. Bender and Stefan Boettcher. "Real Spectra in Non-Hermitian Hamiltonians Having ¡mml:math xmlns:mml="http://www.w3.org/1998/Math/MathML" display="inline"¿ ¡mml:mi mathvariant="bold-script"¿P¡/mml:mi¿ ¡mml:mi mathvariant="bold-script"¿T¡/mml:mi¿ ¡/mml:math¿ Symmetry". In: *Physical Review Letters* 80.24 (1998), pp. 5243–5246. ISSN: 1079-7114. DOI: 10.1103/physrevlett.80.5243. URL: http://dx.doi.org/10.1103/PhysRevLett.80.5243.

[2] A. Guo et al. "Observation of $\mathcal{PT}$-Symmetry Breaking in Complex Optical Potentials". In: *Phys. Rev. Lett.* 103 (9 Aug. 2009), p. 093902. DOI: 10.1103/PhysRevLett.103.093902. URL: https://link.aps.org/doi/10.1103/PhysRevLett.103.093902.

[3] Carl M. Bender, Dorje C. Brody, and Markus P. Müller. "Hamiltonian for the Zeros of the Riemann Zeta Function". In: *Phys. Rev. Lett.* 118 (13 Mar. 2017), p. 130201. DOI: 10.1103/PhysRevLett.118.130201. URL: https://link.aps.org/doi/10.1103/PhysRevLett.118.130201.

[4] Carl M Bender et al. "Complex WKB analysis of energy-level degeneracies of non-Hermitian Hamiltonians". In: *Journal of Physics A: Mathematical and General* 34.6 (Feb. 2001), p. L31. DOI: 10.1088/0305-4470/34/6/101. URL: https://doi.org/10.1088/0305-4470/34/6/101.

[5] Prof. Fabian Hassler. *Lecture Notes Quantum Mechanics*. RWTH Aachen University, 2024.

[6] Per Olaf Fröman Nanny Fröman. "JWKB Approximation Contributions to the Theory". In: (1965).

[7] Carl M Bender. "Making sense of non-Hermitian Hamiltonians". In: *Reports on Progress in Physics* 70.6 (May 2007), pp. 947–1018. ISSN: 1361-6633. DOI: 10.1088/0034-4885/70/6/r03. URL: http://dx.doi.org/10.1088/0034-4885/70/6/R03.

[8] Carl M. Bender and Daniel W. Hook. "$\mathcal{PT}$-symmetric quantum mechanics". In: *Rev. Mod. Phys.* 96 (4 Oct. 2024), p. 045002. DOI: 10.1103/RevModPhys.96.045002. URL: https://link.aps.org/doi/10.1103/RevModPhys.96.045002.

Acknowledgements

First I want to thank Fabian Hassler and Steven Kim for supervising this work. The weekly, inspiring talks with Fabian Hassler and the good guidance from Steven Kim have helped me to find my way through this first project.

Additionally, I want to thank Lennart Sauer, Sinan Blanck, Yusuf Yilmaz, Bastian Seibel and Friedrich Kurth for the company during the long hours and more or less productive talks.

I also want to thank my family and friends for the support they gave me during this time.

Declaration on the use of Artificial Intelligence

In this work artificial intelligence was used to support with the creation of python scripts. Furthermore, artificial inteligence was used to find grammar and spelling mistakes in the thesis itself.